Dear reviewer,

Thank you for taking time to review our manuscript.
We studied your comments and revised our draft accordingly.
We also went through our manuscript and made corrections on the texts.
Changes to the texts were marked in the manuscript and were presented as follows.
Hope that our revised draft will meet with your approval.

Best wishes,
Qinchuan Xin

Anonymous Referee # 1

The study provided by Q. Xin et al "A time-stepping scheme to simulate leaf area index, phenology, and gross primary production across deciduous broadleaf forests in eastern United States" is mainly focused on development of a new modeling algorithm to parameterize the temporal LAI and GPP variability and its application to describe the spatial patterns of LAI, GPP and phenological properties of deciduous broadleaf forests across eastern United States. Adequate parameterization of land surface and vegetation properties is a very important scientific task for modern biogeochemistry. New algorithms can be very useful to solve different applied problems related to adequate description of the land surface - atmosphere interaction in different spatial and temporal scales.

In the paper authors showed new modeling results and their comparison with data obtained using previously developed approaches. Obtained new results however didn't show any significant accuracy improvement in GPP estimations. The difference between measured (derived from measured NEE) and simulated GPP (fig. 3) is still very high.

Reply: Thank you for your comments. This study does not try to improve the GPP simulation but tries to develop a method that can use climate variables to simulate both LAI and GPP. For land surface models that predict GPP values, they require either satellite-derived LAI data or an independent phenology sub-model. The main idea for this study is to improve the phenology modeling by providing time series of LAI simulated using climate variables. Because here we implement the MOD17 algorithm instead of the sophisticated process-based model for the purpose of model simplicity, we have no expectation that the GPP simulated based on model-simulated LAI could be more accurate than the GPP simulated based on satellite-observed LAI.

To address your concern, we add sentences to main texts in the discussion part as follow:
Land surface models that predict vegetation GPP require either satellite-derived LAI input data or the phenology sub-model. The main idea for this study is to improve the phenology modeling by providing time series of LAI simulated using climate variables, and hence enables to simulate GPP forced only by climate variables. Because we implement the MOD17 algorithm instead of the sophisticated

process-based model for the purpose of simplicity, one should not expect that GPP simulated based on the model-simulated LAI could be more accurate than GPP simulated based on the satellite-derived LAI.

Other point for discussion is model assumptions used in the study. In particular authors assumed a linear relationship between the steady-state LAI and the corresponding GPP. However in reality the GPP is non-linearly depended on LAI (not only on total LAI but even on LAI of green biomass) mainly due to non-linear PAR (photosynthetically active radiation) interception within a plant canopy. Such effects are especially pronounced in dense plant canopies with a high LAI. GPP rate is linked with forest and tree architecture. The leaf photosynthesis properties are also varied among different vegetation types. The assimilation rate is depended on biophysical properties of individual plants, water availability, nutrient supply, etc. So, the correctness of made assumption in the study is not obvious and it needs additional discussion.

Reply: We agree with your comments that additional discussion is needed. We conducted an experiment and added paragraphs in the discussion to show the relationship between leaf area index and other variables on the monthly basis. Note that our modeling approach does not try to model GPP based on LAI, but tries to model LAI as a function of GPP. This provides another key function to close the equation systems such that two unknown variables (i.e., LAI and GPP at the steady state) in two independent equations can then be solved numerically. The added paragraphs in the discussion are as follows:

Figure 8 further illustrate the relationship between mean LAI and different variables on a monthly basis. All data were averaged to the monthly time scale such that canopy LAI can be considered as nearly the steady state. On the monthly basis, mean LAI has a strong near-linear relationship with mean GPP (R^2=0.888) and the slope for the regression without intercept is 0.580, the same as we used in the model simulation. On the monthly basis, mean LAI is strongly correlated with mean temperature (R^2=0.799), indicating that temperature is the dominate factor that determines vegetation phenology. Factors like vapor pressure deficit and photoperiod also have positive relationships with mean LAI on the monthly basis. Figure 8 suggests that the processes of leaf phenology and photosynthetic phenology for deciduous broadleaf forest are closely related. Our modeling approach that links canopy GPP with LAI reflects the empirical positive relationship found in Figure 8a.

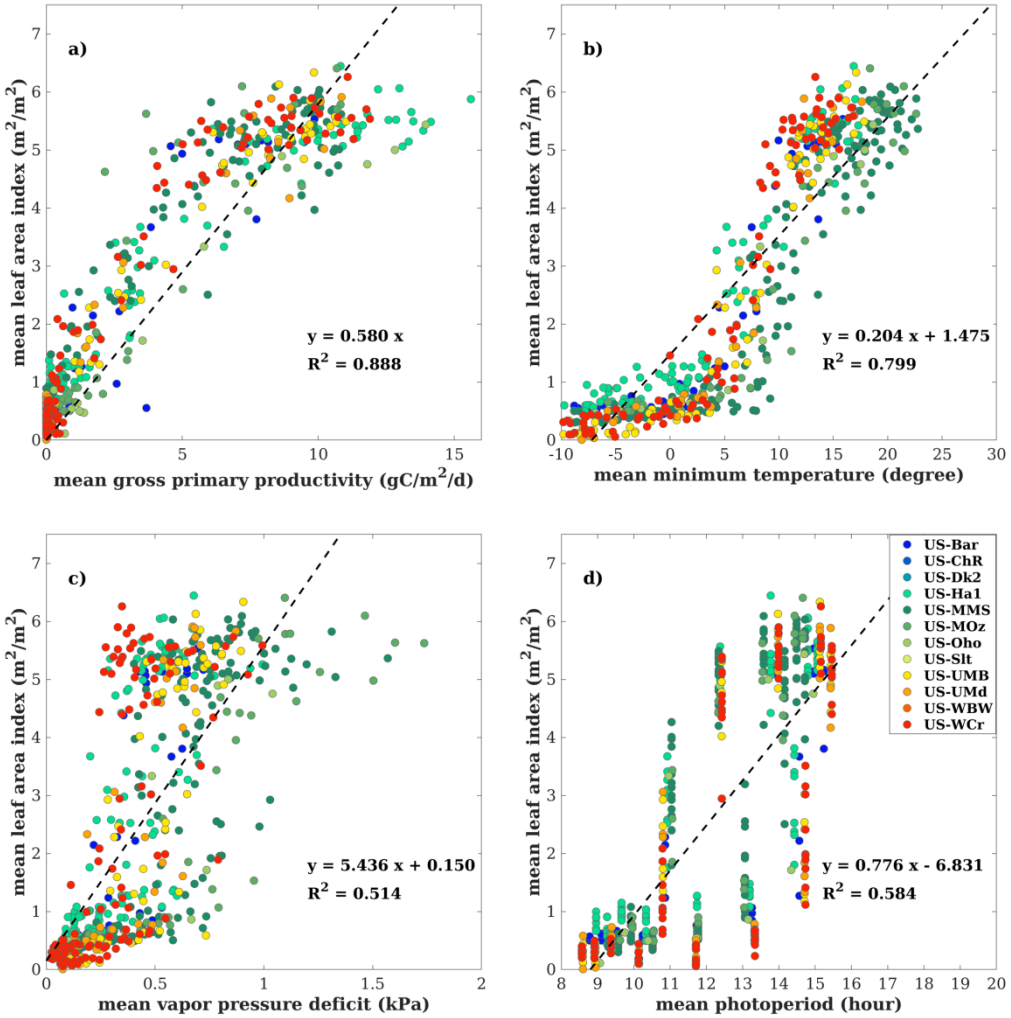

Figure 8: Scatter plots are shown for the relationship a) between mean leaf area index and mean gross primary production, b) between mean leaf area index and mean temperature, c) between mean leaf area index and mean vapor pressure deficit, and d) mean leaf area index and mean photoperiod on a monthly basis. All available site-year flux tower data were included in the analysis. All data were averaged to the monthly time scale for analysis. The dashed lines denote the regression lines. Figure 8a uses the regression without intercept.

Authors pointed out in result chapter about a gut agreement between leaf phenology derived by new method and MODIS data. It is true. But it is not clear from the paper the reasons for available differences between tower observed time of foliage expansion (indicated in shape of black GPP curve) and corresponding time predicted by developed model (fig 1 a-b, page 11)? The model actually predicts earlier leaf onset in spring than in situ observation (GPP data).

Reply: Thank you for pointing out that the model actually predicts earlier leaf onset in spring than in situ observation in terms of the GPP data. We suspect that the flux tower GPP data as shown in the figure suffer from instrument malfunction, because the GPP data increased sharply and unreasonably within very short time in the spring time. To avoid the confusion, we update the figure using data from US-UMB in 2004.

The updated figure looks as follows:

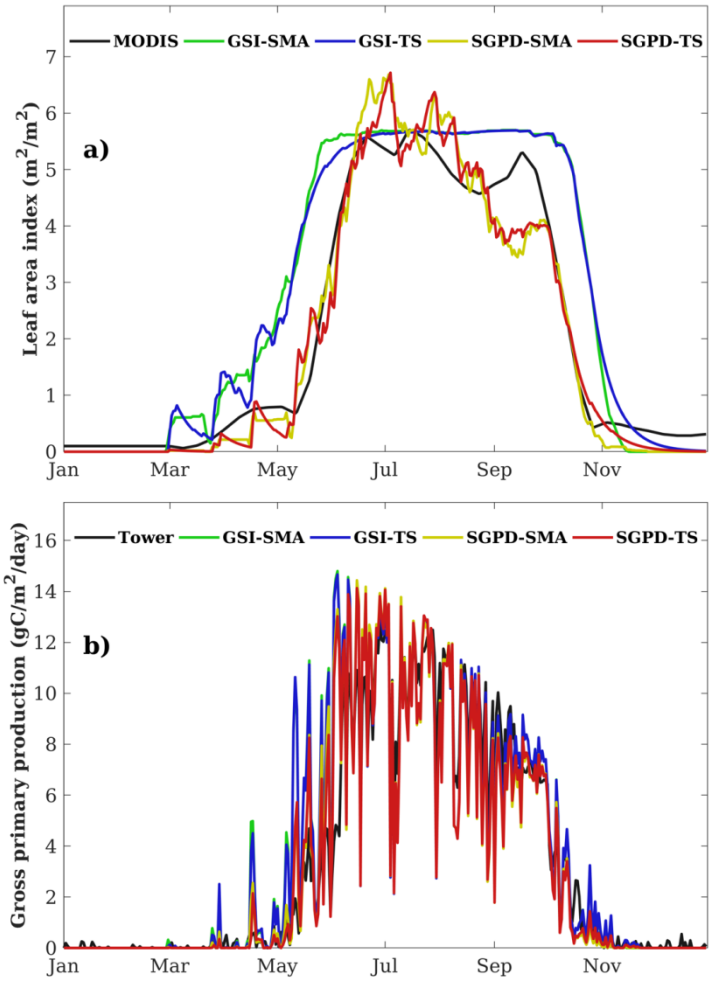

Figure 1: The modeled and measured daily time series of a) leaf area index and b) gross primary production are shown for the flux tower site of US-UMB in 2004. The reference LAI time series in Figure 1a are derived from the MODIS data and the reference GPP time series in Figure 1b are obtained from the flux tower measurements.

In the first half of introduction authors used many well known statements such as e.g. "energy and mass exchange in a plant canopy can be modeled as a function of environmental conditions (e.g., sunlight, soil moisture, temperature, and humidity) and vegetation LAI "and refereed them to most recent own publications only, and not to available synthesis studies conducted during the last several decades and focused on the same problem.

Reply: Thank you for your comments. We removed the self-cited references and added some recent studies to the texts as follows:

Hufkens, K., Basler, D., Milliman, T., Melaas, E. K., and Richardson, A. D.: An integrated phenology modelling framework in R, Methods in Ecology and Evolution, 9, 1276-1285, 2018.

Li, W., Guo, Q., Tao, S., and Su, Y.: VBRT: A novel voxel-based radiative transfer model for heterogeneous three-dimensional forest scenes, Remote Sensing of Environment, 206, 318-335, 2018.

Liu, Q., Fu, Y. H., Liu, Y., Janssens, I. A., and Piao, S.: Simulating the onset of spring vegetation growth across the Northern Hemisphere, Global change biology, 24, 1342-1356, 2018.

Yuan, H., Dickinson, R. E., Dai, Y., Shaikh, M. J., Zhou, L., Shangguan, W., and Ji, D.: A 3D Canopy Radiative Transfer Model for Global Climate Modeling: Description, Validation, and Application, Journal of Climate, 27, 1168-1192, 2013.

I find that the discussion chapter is too short. It should be extended. All obtained results have to be discussed in more details.

Reply: Thank you for your comments. We agree that the discussion chapter should be extended. Based on other comments, we further discussed the relationship between leaf area index and other climate variables and we discussed the model limitations. Please find our responses mentioned above and in the manuscript for details to changes in the discussion chapter.

The sentence in page 4 is not clear "leaf dynamics takes days or even months in response to climate variation". I guess authors mean weather not climate variations. Time scale for climate variation is much larger.

Reply: We agree that using the word “weather” is precise. We revised the sentence as “Unlike leaf photosynthesis that approaches equilibrium within a minute and stomatal functioning that reaches the steady state in minutes (Sellers et al., 1996a), leaf dynamics takes days or even months in response to weather variation (Zeng et al., 2013).”

I’m not agreed also that the term potential evapotranspiration assumes the fixed LAI (page 3) for any hypothetic canopy. Fixed LAI can be obviously used for calculation of "reference evapotranspiration" but not potential evapotranspiration. Potential evapotranspiration rate can be estimated for plant canopy with different LAI values.

Reply: Thank you for your comments. We agree that using “reference evapotranspiration” is more accurate than using “potential evapotranspiration”. Note that some researchers still use “potential evapotranspiration” in their publications as the term “potential evapotranspiration” is easy to understand. Based on your suggestions, we revised the sentence as “Analogous to the method that derives reference evapotranspiration, the developed method defines a hypothetic canopy with fixed LAI to model potential GPP under certain environment conditions.”

A simple time-stepping scheme to simulate leaf area index, phenology, and gross primary production across deciduous broadleaf forests in eastern United States

Qinchuan Xin [1], Yongjiu Dai [2], Xiaoping Liu [1]

[1]Guangdong Key Laboratory for Urbanization and Geo-simulation, Sun Yat-sen University, Guangzhou 510275, China
[2]School of Atmospheric Sciences, Sun Yat-sen University, Guangzhou 510275, China

Correspondence to: Qinchuan Xin (xinqinchuan@gmail.com); Yongjiu Dai (daiyj6@mail.sysu.edu.cn)

Abstract. Terrestrial plants play a key role in regulating the exchange of energy and materials between the land surface and the atmosphere. ~~Robust t~~Terrestrial biosphere models that simulate ~~both time series of~~ leaf dynamics and canopy photosynthesis are required to understand the vegetation-climate interactions. This study proposes a simple time stepping scheme to simulate leaf area index (LAI), phenology, and gross primary production (GPP) ~~simultaneously via only~~when forced with climate variables ~~based on an ecological assumption that plants allocate leaf biomass till an environment could sustain to maximize photosynthetic reproduction~~. The method establishes a linear function between the steady-state LAI and the corresponding GPP, which is used to track the suitability of environmental conditions for plant photosynthesis. The method ~~, and~~ applies the established function and the MOD17 algorithm to form simultaneous equations together, which can be solved numerically. To account for the ~~time lags in plant responses of leaf allocation to environment variation~~time-lagged responses of plant growth to environmental conditions, a time stepping scheme is developed to simulate the LAI time series based on the solved steady-state LAI. The simulated LAI time series is then used to derive the timing of key phenophases and simulate canopy GPP with the MOD17 algorithm. The developed method is applied to deciduous broadleaf forests in eastern United States and has found to perform well on simulating canopy LAI and GPP at the site scale as evaluated using both flux tower and satellite data. The method could also capture the spatiotemporal variation of vegetation LAI and phenology across eastern United States as compared with satellite observations. The developed time-stepping scheme provides a simplified and improved version of our previous modeling approach and forms a potential basis for regional to global applications in future studies.

1 Introduction

Terrestrial plants play a key role in regulating the exchange of energy and materials (e.g., radiation, heat and moisture, carbon, and trace gas fluxes) between the land surface and the atmosphere (Beer et al., 2010; Zhu et al., 2017). The canopy structures and characteristics govern solar radiation interception and absorption ~~as well as momentum flows on the land surface~~ (Ni-Meister et al., 2010; Yuan et al., 2013). ~~Individual p~~Plants control water transpiration and photosynthetic carbon

fixation through processes from transient changes in leaf stomatal conductance to seasonal variation in foliage dynamics (Eagleson, 2005). In turn, external environmental conditions, such as sunlight, temperature, and water and nutrient availability, selectively determine plant form and function (Bonan, 2008). Numerical terrestrial biosphere models that integrates multidisciplinary knowledges of the Earth sciences is an essential toolallow to understand and predict the interactions between terrestrial ecosystems and the climate under a changing global environment.

To match the atmosphere circulation models, dDevelopments on the terrestrial biosphere models essentially seek accurate representation as well as the solution to the simulation of energy and material exchanging fluxes between ecosystems and the atmosphere. In terrestrial biosphere models, plant canopies are typically characterized using leaf area index (LAI; leaf area per unit ground area) because plant leaf is the basic organ that intercepts solar radiation for photosynthesis and transpiration (Li et al., 2018; Yuan et al., 2013). The exchanging fluxes of energy and materials over vegetation canopy can then be modeled as a function of environmental conditions (e.g., sunlight, soil moisture, temperature, and humidity) and vegetation LAI (Ding et al., 2014). The As the vigorous development of satellite remote sensing technology offers large-scale observations for vegetation monitoring and, a number of modeling approaches have been developed to quantify and simulate the land surface fluxes based on climate variables and satellite-derived LAI. These methods, including both the light use efficiency models (e.g., the Carnegie-Ames-Stanford Approach (CASA) model (Potter et al., 1993), the MOD17 algorithm (Running et al., 2004), the Vegetation Photosynthesis Model (VPM) (Xiao et al., 2004), the eddy covariance light use efficiency (EC-LUE) model (Yuan et al., 2010), and the two-leaf light use efficiency (TL-LUE) model (He et al., 2013)) and the process-based models (e.g., the boreal ecosystem productivity simulator (BEPS) model (Liu et al., 1997), the Breathing Earth System Simulator (BESS) model (Ryu et al., 2011), the Growing Production-Day (GPD) model (Xin, 2016), the revised Simple Biosphere (SiB2) model (Sellers et al., 1996b)), despite differing from each other on the representation of vegetation processes, have been successfully used for applications from field to global scales. While remote sensing data of vegetation activities perfectly complements the canopy process models, developing the sub-model that could simulate the dynamics of vegetation LAI is fundamental to enhance our abilities on predicting terrestrial ecosystem processes under future scenarios.

Modeling vegetation leaf dynamics via climate variables requires in-depth understanding on plant phenology,phenological processes. of which the This modeling is still largely empirical to date and contributes considerable uncertainties to current terrestrial biosphere models (Richardson et al., 2012). One common method for simulating vegetation phenology is to predict the timing of key phenophases such as spring onset and autumn senescence in a growing season (Hufkens et al., 2018; Liu et al., 2018). For example, most phenology models originate from the Growing Degree Day (GDD) model, a method first proposed by De Réaumur dating back to 1735 (De Réaumur, 1735). The GDD model assumes that plant leaf onset begins when daily mean temperatures accumulated from a fixed date reach a critical threshold. Studies have identified that various environmental factors other than temperature could affect plant phenology to certain degrees (Polgar and Primack,

2011), and therefore, efforts have been made to improve the GDD model by adding different influential factors, such as photoperiod, soil temperature, humidity, and soil moisture (Chuine et al., 1999; Hufkens et al., 2018; Liu et al., 2018; Melaas et al., 2013; Yang et al., 2012). Land surface models like the Community Land Model (Oleson et al., 2013) and the Biome-BGC model (White et al., 2000) use a set of complicated and empirical equations to predict the timing of key phenophases across plant functional types. Another method for vegetation phenology modeling is to simulate the entire LAI time series over a growing season. For example, the DeNitrification DeComposition model uses an optimal seasonal growth curve of plant LAI and then calculates environmental stresses of water and nitrogen to limit daily carbon and nitrogen allocation to plant leaves~~leaf biomass allocation~~ (Yu et al., 2014). The Growing Season Index as proposed by (Jolly et al., 2005) is a widely used method that could simulate seasonal phenology curves using the climate variables of photoperiod, air temperature, and vapor pressure deficit. While these studies have greatly ~~enriched the availability~~benefitted the development of the phenology models, there is still a need to improve the current phenology models. ~~the current development of the vegetation phenology models encounters a dilemma: adding different influential climate variables to account for their impacts on leaf dynamics seems inevitable but certainly complicates the model structure and does not always improve the model accuracies consistently across space and time.~~

~~While most of the existing studies choose to develop the plant phenology model independently from the canopy flux model, the~~ The physiological processes of leaf ~~distribution~~ phenology and canopy photosynthesis are interrelated. Plants absorb carbon dioxide to accumulate biomasses through photosynthesis and then redistribute the photosynthetic gain to organs such as leaves, roots, and stems to optimize reproduction. Given limited external resources, plants have evolved to effectively allocate ~~the leaf biomass~~photosynthate to organs in response to environment ~~variation~~ conditions so as to maximize photosynthetic carbon gain, the fundamental bioenergy for survival (Givnish, 1986). The strategy of biomass allocation among growth, maintenance, and reproduction in a continuously changing environment directly determines whether plants could persist under natural competition pressures from both inter- and intra-species (Bonan, 2002). In essence, there is a need to synthesize~~d~~ the analysis of both canopy photosynthesis and leaf ~~distribution~~ phenology processes ~~is needed to solve the difficulties in the development of the current terrestrial biosphere models~~.

~~Targeting the current problems associated with vegetation phenology modeling,~~ (Xin, 2016) ~~first~~ proposed a parameterization scheme to simulate vegetation productivity and phenology simultaneously. The method, named as the Growing Production Day (GPD) model, uses canopy gross primary production (GPP) instead of air temperature as an indicator that synthesizes various environmental factors on plant photosynthesis to track how the environment is suitable for vegetation growth. Analogous to the method that derives ~~potential~~ reference evapotranspiration, the developed method defines a hypothetic canopy with fixed LAI to model potential GPP ~~(or reference GPP to be precise)~~ under certain environment conditions. Similar to the GDD model, the GPD model predicts vegetation spring onset to occur when the accumulated reference GPP reaches a critical threshold. The method has been successfully applied to the biomes of

evergreen needleleaf forest, deciduous broadleaf forest, and grassland. To allow for predicting the entire LAI time series over a growing season, (Xin et al., 2018) further improved the GPD model by proposing a linear function between LAI and GPP at the steady state. The proposed function and the sophisticated canopy GPP model (i.e., modeling GPP as a function of LAI and climate variables) together form ~~establishing~~ a closed system of equations that includes both vegetation GPP and LAI. The improved GPD model ~~first solves~~ uses the numerical approach, a method that gives an initial value and then iterates to the convergence of the solution, to solve the closed system of equations ~~numerically to~~ and derives LAI in the steady state~~and~~. The improved GPD model then applies the simple moving average method to the steady-state LAI to obtain the modeled LAI time series. The improved method circumvents the need to empirically prescribe a fixed canopy and enables modeling of LAI time series in addition to the timing of individual phenophases. There remain shortcomings to overcome for the broad applications of the GPD model. First, the simple moving average method, despite being widely used in many studies, is empirical and does not match with the land surface models that commonly operate at incremental time steps. Second, the developed GPD model that includes many subtle vegetation processes, such as canopy radiative transfer, leaf stomatal conductance, leaf transpiration, leaf photosynthesis, and soil evaporation, is computationally intensive and requires various climate input data ~~that are often not readily available for regional to global simulations~~.

Aiming to solve the above-mentioned problems, the objectives of the study are to: 1) develop a time stepping scheme to simulate leaf dynamics and vegetation productivity, and 2) simplify the GPD model to allow for long-term applications at a large scale. Given that the phenology modeling in deciduous broadleaf forest, a biome that have distinct seasonal growing cycles, still has large uncertainties (Melaas et al., 2016), this study choose to simulate the deciduous broadleaf forests across the eastern United States such that the developed method if successful could provide a potential basis for future applications to other biomes.

2 Methods and materials

2.1 Modeling steady-state leaf area index

One difficulty in vegetation phenology modeling is that the time scale associated with leaf allocation far exceeds that of many other vegetation processes. Unlike leaf photosynthesis that approaches equilibrium within a minute and stomatal functioning that reaches the steady state in minutes (Sellers et al., 1996a), leaf dynamics takes days or even months in response to ~~climate~~ weather variation (Zeng et al., 2013). (Xin et al., 2018) first put forward the concept of the steady-state leaf area index, i.e., canopy LAI when time approaches infinity while the environmental conditions remain unchanging. An alternative biological explanation to the steady-state LAI is the maximum canopy LAI that an environment can sustain infinitely by its own photosynthetic activities. Supposing that the carrying capacity of canopy LAI is proportional to total canopy photosynthetic rate under a given environment, the steady-state LAI can be modeled as follows:

$$LAI_s = mGPP_s \quad (1)$$

where LAI_s denotes the steady-state leaf area index; m denotes the constant ratio of steady state leaf area index to environmental capacity; and GPP_s denotes the steady-state gross primary production.

The above equation, despite having a simple form, provides a critical function that complements the canopy photosynthesis model. The only parameter m is dependent on plant functional type and can be quantified from field measurements as the average ratio of LAI to GPP at canopy closure (i.e., the time when both canopy LAI and GPP reach equilibrium). Studies have developed various canopy photosynthesis models, such as the light use efficiency models and the process-based models. Our previous studies (Xin, 2016; Xin et al., 2018) implemented a sophisticated canopy model that assembles the sub-models of canopy radiative transfer, leaf stomatal conductance, leaf transpiration, soil evaporation, and leaf photosynthesis. Although the method has been successfully applied to different biomes, the model structure is complicated for studies at the regional to global scales. To simulate canopy photosynthesis, this study implements the MOD17 algorithm, a big-leaf light use efficiency model that ~~is used to provide~~uses routine satellite products (Running et al., 2004). The use of the MOD17 algorithm could greatly simplify the modeling processes and reduce the required climate variables, thereby allowing for broad applications. A brief description on the MOD17 algorithm is provided here where details can be found from the user guide of the MODIS GPP product (Running and Zhao, 2015).

Based on the MOD17 algorithm, vegetation GPP can be modeled as follows:

$$GPP_s = PAR \times FPAR \times \varepsilon_{max} \times f(T) \times f(VPD) \quad (2)$$

where GPP_s denotes the steady-state gross primary production; PAR denotes photosynthetically active radiation; FPAR denotes the fraction of photosynthetically active radiation; ε_{max} denotes maximum light use efficiency; and $f(T)$ and $f(VPD)$ denote the scalar functions that account for the limitation of temperature and vapor pressure deficit, respectively, on canopy photosynthesis.

The fraction of photosynthetically active radiation can be modeled as follows (Turner et al., 2006):

$$FPAR = 1 - \exp(-kLAI_s) \quad (3)$$

where k denotes the canopy light extinction coefficient and LAI_s denotes the steady-state leaf area index.

The environmental scalars can be modeled as follows:

$$f(T) = \max\left(\min\left(\frac{TMIN - TMIN_{min}}{TMIN_{max} - TMIN_{min}}, 1\right), 0\right) \quad (4)$$

$$f(\mathrm{VPD}) = \max\left(\min\left(1 - \frac{\mathrm{VPD} - \mathrm{VPD_{min}}}{\mathrm{VPD_{max}} - \mathrm{VPD_{min}}}, 1\right), 0\right) \quad (5)$$

where TMIN denotes daily minimum air temperature; $\mathrm{TMIN_{min}}$ and $\mathrm{TMIN_{max}}$ denote the lower and upper thresholds of daily minimum air temperature for vegetation photosynthetic activities, respectively; VPD denotes daily vapor pressure deficit; and $\mathrm{VPD_{min}}$ and $\mathrm{VPD_{max}}$ denote the lower and upper thresholds of daily vapor pressure deficit for vegetation photosynthetic activities, respectively.

Given the environmental conditions, Equations 1 and 2 together form simultaneous equations, meaning that there are two unknown variables (i.e., LAI and GPP at the steady state) and two different general equations. One may derive an analytic solution if both equations have simple forms. But because the dependence of GPP on LAI is non-linear, deriving the analytic solution is complicated and we could apply the numerical approach to obtain the solutions. Because $\mathrm{LAI_s}$ increases as a linear function of $\mathrm{GPP_s}$ in Equation 1 and $\mathrm{GPP_s}$ increases as a logarithmic function of $\mathrm{LAI_s}$ in Equation 2, the simultaneous equations have one and only one nonzero solution of $\mathrm{LAI_s}$. ~~The nonzero solution can be obtained by implementing a~~ To obtain the nonzero solution, the numerical approach ~~that~~ starts with a ~~given initial~~ guess value of $\mathrm{LAI_s}$ and then ~~solves the equations iteratively~~ then iterates to obtain the approximated solution of $\mathrm{LAI_s}$ until converging. Note that the numerical approach is widely used in the land surface models. For example, as the stomatal resistance, the CO2 partial pressure at the leaf surface, the internal leaf CO2 partial pressure, and the leaf net photosynthesis are dependent on each other, the Community Land Model 4.5 uses the numerical approach to solve stomatal resistance and leaf photosynthesis iteratively until the internal leaf CO2 partial pressure converges.

2.2 Modeling leaf area index, phenology, and gross primary production

Because the physiological processes that plants allocate photosynthates to leaves ~~Because the physiological processes that plants allocate leaf biomass~~ do not respond instantaneously to climate variation, there is a need to simulate vegetation LAI as lagging behind the steady state. One method to account for the time lagging effect is to apply the simple moving average method to buffer abrupt changes from individual events in the time series. Our previous study applied the simple moving average method to model LAI as the unweighted mean of the previous $\mathrm{LAI_s}$ as follows (Xin et al., 2018):

$$\mathrm{LAI} = \frac{1}{\mathrm{n_{day}}} \sum_{\mathrm{i}=0}^{\mathrm{n_{day}}-1} \mathrm{LAI_s} \quad (6)$$

where LAI denotes leaf area index at the n day; $\mathrm{n_{day}}$ denotes the number of days; i denotes an index starting from 0 to $\mathrm{n_{day}} - 1$; and $\mathrm{LAI_s}$ denotes the steady state leaf area index.

The simple moving average method, while showing useful in vegetation phenology modeling, is suitable for retrospective analysis rather than prediction, and importantly, it does not match with most land surface models that operate at incremental time steps. Analogous to the method used to simulate leaf stomatal conductance in response to environmental variation, this study proposes a time stepping scheme to simulate LAI realistically as lagging behind the steady state by a simple restricted growth model (Sellers et al., 1996a) as follows:

$$\frac{dLAI}{dt} = k_l(LAI_s - LAI) \quad (7)$$

where t denotes the time; k_l denotes a time constant that reflects the responses of plant leaf allocation to climate variation; and LAI and LAI_s denote the leaf area index and the steady state leaf area index, respectively.

In the time stepping scheme, vegetation LAI does not change much during winter or summer as the current LAI is close to LAI_s, whereas vegetation LAI increases (or decreases) during spring (or autumn) as the current LAI is less (or greater) than LAI_s. For example, when the environment turns favorable for plant growth in spring, LAI_s exceeds LAI and $dLAI/dt$ is positive such that the modeled canopy LAI increases. Note that the method developed here essentially uses the canopy photosynthetic capacity (i.e., the steady-state gross primary production) instead of air temperature as a synthesized indicator to track the suitability of the environment to plant growth in time series, and therefore, the developed method is referred to as the Simplied Growing Production-Day (SGPD) model following our previous studies (Xin et al., 2018).

Given the modeled LAI time series, both vegetation phenology and canopy GPP can be easily ~~retrieved~~modeled (Xin et al., 2018). Various approaches have already been developed to derive the timing of key phenophases such as spring onset and autumn senescence from seasonal LAI trajectories. This study models the phenological transition dates using a simple method that derives the first spring and last autumn dates at which LAI reaches 20%, 50%, and 80% of the seasonal amplitudes (Richardson et al., 2012). The selected relative amplitudes (20%, 50%, and 80%) are correspondent to different plant growth stages over a growing season. Because the MOD17 algorithm only requires LAI, daily minimum temperature, daily vapor pressure deficit, and daily photosynthetically active radiation as model inputs, ~~Given temperature and vapor pressure deficit,~~ the canopy GPP is simply modeled by substituting the modeled LAI time series and the climate variables ~~back~~ into the MOD17 algorithm. For the first day of spring when the LAI is zero, the modeled GPP is zero. As times move forward, the modeled GPP increases as LAI increases but is still dependent on other climate variables such as solar radiation, temperature and vapor pressure deficit.

2.3 Comparative studies using Growing Season Index

The Growing Season Index (GSI), a widely used method in vegetation phenology modeling~~, allows for modeling seasonal LAI time series rather than individual phenophases and is implemented to make direct comparisons with the SGPD model~~ (Jolly et al., 2005), allows for modeling seasonal LAI time series rather than individual phenophases and is implemented to

make direct comparisons with the SGPD model. The GSI model performs comparably to or even outperforms other terrestrial biosphere models on predicting the timing of key phenophases for deciduous broadleaf forests (Melaas et al., 2013).

The instantaneous GSI is first derived based on the work of (Jolly et al., 2005) as follows:

$$\mathrm{iGSI} = \mathrm{iTMIN} \times \mathrm{iVPD} \times \mathrm{iPhoto} \quad (8)$$

where iGSI denotes instantaneous growing season index; and iTMIN, iVPD, and iPhoto denote the instantaneous scalar functions that account for the constraints of daily minimum air temperature, vapor pressure deficit, and photoperiod, respectively, on vegetation growth.

The scalar functions for iTMIN, iVPD, and iPhoto have the mathematic forms similar to Equations 4 and 5 and are derived the same as defined in (Jolly et al., 2005) as follows:

$$\mathrm{iTMIN} = \max\left(\min\left(\frac{\mathrm{TMIN} - \mathrm{TMIN_{min}}}{\mathrm{TMIN_{max}} - \mathrm{TMIN_{min}}}, 1\right), 0\right) \quad (9)$$

$$\mathrm{iVPD} = \max\left(\min\left(1 - \frac{\mathrm{VPD} - \mathrm{VPD_{min}}}{\mathrm{VPD_{max}} - \mathrm{VPD_{min}}}, 1\right), 0\right) \quad (10)$$

$$\mathrm{iPhoto} = \max\left(\min\left(\frac{\mathrm{Photo} - \mathrm{Photo_{min}}}{\mathrm{Photo_{max}} - \mathrm{Photo_{min}}}, 1\right), 0\right) \quad (11)$$

where TMIN denotes daily minimum temperature; $\mathrm{TMIN_{min}}$ and $\mathrm{TMIN_{max}}$ denote the lower and upper thresholds of daily minimum air temperature for vegetation photosynthetic activities, respectively; VPD denotes daily vapor pressure deficit; $\mathrm{VPD_{min}}$ and $\mathrm{VPD_{max}}$ denote the lower and upper thresholds of daily vapor pressure deficit for vegetation photosynthetic activities, respectively; Photo denotes daily photoperiod; and $\mathrm{Photo_{max}}$ and $\mathrm{Photo_{min}}$ denote the lower and upper thresholds of daily photoperiod for vegetation photosynthetic activities, respectively.

LAI can be modeled as the simple moving average of the instantaneous GSI scaled using maximum LAI as follows:

$$\mathrm{GSI} = \frac{1}{\mathrm{n_{day}}} \sum_{\mathrm{i}=0}^{\mathrm{n_{day}}-1} \mathrm{iGSI} \quad (12)$$

$$\mathrm{LAI} = \mathrm{GSI} \times \mathrm{LAI_{max}} \quad (13)$$

where GSI denotes growing season index at the n day; $\mathrm{n_{day}}$ denotes the number of days; i denotes an index starting from 0 to the previous one day; iGSI denotes the instantaneous growing season index; and $\mathrm{LAI_{max}}$ denotes the maximum leaf area index at canopy closure.

It is noteworthy that the instantaneous GSI uses the product of the scalars of minimum temperature, vapor pressure deficit, and photoperiod as an indicator to track the potential canopy photosynthetic capacities on the daily basis. Both the GSI model and the SGPD model, despite having different forms, share the same modeling idea. To understand the differences between the simple moving average method and the time stepping method, the GSI model is also implemented with the simple restricted growth model as follows:

$$\mathrm{LAI_s} = \mathrm{iGSI} \times \mathrm{LAI_{max}} \tag{14}$$

$$\frac{\mathrm{dLAI}}{\mathrm{dt}} = \mathrm{k_l}(\mathrm{LAI_s} - \mathrm{LAI}) \tag{15}$$

where iGSI denotes the instantaneous growing season index; $\mathrm{LAI_{max}}$ denotes the maximum leaf area index at canopy closure; $\mathrm{k_l}$ denotes a time constant that accounts for the lagged responses of plant leaf allocation to climate variation; and LAI and $\mathrm{LAI_s}$ denote the leaf area index and the steady state leaf area index, respectively.

With the modeled LAI time series, the phenological transition dates are then retrieved based on the seasonal amplitude ratio method, the same way as processing the LAI time series derived from the SGPD model. Vegetation GPP is modeled by substituting the modeled LAI time series into the MOD17 algorithm.

2.4 Model comparison and parameterization

This study compares four different modeling approaches, including the results simulated using both the SGPD model and the simple moving average method (hereinafter referred to as SGPD-SMA), using both the SGPD model and the time stepping scheme (hereinafter referred to as SGPD-TS), using both the GSI model and the simple moving average method (hereinafter referred to as GSI-SMA), and using both the GSI model and the time stepping scheme (hereinafter referred to as GSI-TS). The commonly used metrics, including the Pearson correlation coefficient (R), the coefficient of determination (R^2), the root-mean-square error (RMSE), and the mean bias error (MBE), are derived for model assessment and comparison.

As the MOD17 algorithm is a well-parameterized model, this study applies the model parameters from literature directly. Following the user guide of the MODIS GPP product (Running and Zhao, 2015), key parameters in the MOD17 algorithm are set as $\varepsilon_{max} = 1.165\ \mathrm{gC/MJ}$, $\mathrm{TMIN_{min}} = -6.0\ ^{\circ}\mathrm{C}$, $\mathrm{TMIN_{max}} = 9.94\ ^{\circ}\mathrm{C}$, $\mathrm{VPD_{min}} = 0.65\ \mathrm{kPa}$, and $\mathrm{VPD_{max}} = 1.65\ \mathrm{kPa}$. The light extinction coefficient of the canopy is 0.5. The parameter that defines the ratio of leaf area index to environmental capacity is set as $\mathrm{m} = 0.58\ \mathrm{m^2(leaf\ area)/gC/day}$ as quantified using the average ratio of LAI to GPP at canopy closure using the flux tower data. The canopy maximum LAI is set as 5.80 based on the maximum 95th percentile of satellite-derived LAI across sites and years (Xin et al., 2018). The parameter $\mathrm{n_{day}}$ in the simple moving average method and the

parameter k_l in the time stepping method control the response of plant leaf allocation to environmental variation. The parameter n_{day} is set as 21 days and the parameter k_l is calibrated as 0.080 day^{-1}.

~~2.4~~2.5 Study materials and pre-processing

~~Our modeling studies are made~~ We evaluate our approach at the site scale using both the flux tower data and remote sensing data and at the regional scale using both the climate data and remote sensing data for deciduous broadleaf forests in eastern United States. ~~In~~ For the site-scale studies, all the flux tower sites of deciduous broadleaf forests (Table 1) that are available in the AmeriFlux website (http://ameriflux.ornl.gov/) were used for analysis. As the developed SGPD model is a simplified version of our previous modeling approach, the site-scale modeling studies only require daily incoming solar radiation, minimum air temperature, vapor pressure deficit, photoperiod, LAI, and GPP data. Daily incoming solar radiation, vapor pressure deficit, and GPP have already been provided in the Level 4 flux tower data, whereas daily minimum air temperature was processed from the half-hourly gap-filled Level 2 data and daily photoperiod as required by the GSI model was computed based on Equation 13 as a function of geolocation and the day of year (Allen et al., 1998). As the MODIS LAI has been found to match field measurements well for deciduous broadleaf forests in eastern United States (Myneni et al., 2002), the 8-day 500 m MODIS LAI Version 6 products (MOD15A2H) that are downloaded from the Land Processes Distributed Active Archive Center (https://lpdaac.usgs.gov/) were used as the reference data. Canopy LAI at each site were extracted from MOD15A2H for the pixel that contains the corresponding site. The extracted 8-day MODIS LAI if identified as poor quality in MOD15A2H were replaced using the three-point median-value moving window technique. Spikes in the LAI time series were removed using the Hampel filter and then gap-filled using the autoregressive modeling approach (Akaike, 1969). The obtained 8-day LAI time series were further smoothed using the Savitzky-Golay filter and then linearly interpolated to generate daily time series. The phenological transition dates were retrieved from daily LAI time series using the method that derives the first spring and last autumn dates at which LAI reaches 20%, 50%, and 80% of the seasonal amplitudes, respectively (Richardson et al., 2012).

$$\mathrm{Pho} = \frac{24}{\pi}\arccos\left(-\tan(\varphi)\tan\left(0.409\sin\left(\frac{2\pi}{365}\mathrm{DOY} - 1.39\right)\right)\right) \quad (16)$$

where Pho denotes daily photoperiod; φ denotes the latitude; and DOY denotes the day of year.

Table 1: Site information for the studied flux towers of deciduous broadleaf forests.

Site Code	Site Name	Lat (°N)	Lon (°W)	Elev (m)	Years	Reference
US-Bar	Bartlett Experimental Forest	44.0646	-71.2881	272	2004-2011	Jenkins et al. (2007)
US-ChR	Chestnut Ridge	35.9311	-84.3324	286	2006-2010	Hollinger et al. (2010)
US-Dk2	Duke Forest Hardwoods	35.9736	-79.1004	168	2007-2008	Oishi et al. (2008)
US-Ha1	Harvard Forest EMS Tower	42.5378	-72.1715	340	2000-2012	Urbanski et al. (2007)
US-MMS	Morgan Monroe State Forest	39.3231	-86.4131	275	2000-2014	Dragoni et al. (2011)

US-MOz	Missouri Ozark	38.7441	-92.2000	219	2005-2013	Gu et al. (2006)
US-Oho	Oak Openings	41.5545	-83.8438	230	2005-2011	Xie et al. (2014)
US-Slt	Silas Little Experimental Forest	39.9138	-74.5960	30	2005-2012	Clark et al. (2012)
US-UMB	Univ. of Mich. Biological Station	45.5598	-84.7138	234	2000-2012	Gough et al. (2013)
US-UMd	UMBS Disturbance	45.5625	-84.6975	239	2008-2012	Gough et al. (2013)
US-WBW	Walker Branch	35.9588	-84.2874	343	2000-2006	Miller et al. (2007)
US-WCr	Willow Creek	45.8060	-90.0798	515	2000-2013	Desai et al. (2008)

Our regional-scale studies used both the climate data and satellite remote sensing data from 1982 to 2016. The daily 1000 m Daymet Version 3 dataset (Thornton et al., 2012) was downloaded from the Oak Ridge National Laboratory Distributed Active Archive Center (http://daymet.ornl.gov/). The Daymet dataset provided daily incoming solar radiation, minimum temperature, vapor pressure, and photoperiod data and we derived daily vapor pressure deficit as the difference between average saturated vapor pressure and vapor pressure. Two different satellite LAI products, including the Global Land Surface Satellite (GLASS) dataset (Xiao et al., 2014) spanning from 1982 to 2014 and the MODIS LAI dataset (Myneni et al., 2002) spanning from 2001 to 2016, were used for the regional studies. The 8-day GLASS LAI product was generated at the 0.05° resolution using the AVHRR data for the time period from 1982 to 1999 and at the 1000 m resolution using the MODIS data for the time period from 2000 to 2012. The 8-day satellite LAI data across eastern United States were processed the same way as the processing of the site-scale data to obtain daily LAI time series. Because seasonal LAI amplitudes for each individual pixel could vary from year to year, the 2001-2010 average seasonal LAI amplitude were used as a baseline to derive the start of the season (SOS) and the end of the season (EOS) for each pixel for each year as the dates when seasonal LAI reaches 50% of the multi-year average seasonal LAI amplitude. The growing season length (GSL) was derived as the difference between EOS and SOS. A 500 m MODIS-based land cover map was obtained from the USGS Land Cover Institute (https://landcover.usgs.gov/). The land cover map was generated by choosing the land cover classification with the highest overall confidence for each pixel in 10-year (2001-2010) Collection 5.1 MODIS land cover type (MCD12Q1) data (Broxton et al., 2014). The 500 m land cover map was resampled to 1000 m resolution using the majority resampling approach and was reprojected to the Lambert Conformal Conic projection to mask areas that are not covered by deciduous broadleaf forests.

~~2.5 Model parameterization and comparison~~

~~As the MOD17 algorithm is a well parameterized model, this study applies the model parameters in literature directly. Following the user guide of the MODIS GPP product (Running and Zhao, 2015), key parameters in the MOD17 algorithm are set as $\varepsilon_{max} = 1.165\ gC/MJ$, $TMIN_{min} = -6.0\ °C$, $TMIN_{max} = 9.94\ °C$, $VPD_{min} = 0.65\ kPa$, and $VPD_{max} = 1.65\ kPa$. The light extinction coefficient of the canopy is 0.5. The parameter that defines the ratio of leaf area index to environmental capacity is set as $m = 0.58\ m^2(leaf\ area)/gC/day$ as quantified using the average ratio of LAI to GPP at canopy closure~~

using the flux tower data. The canopy maximum LAI is set as 5.80 based on the maximum 95th percentile of satellite-derived LAI across sites and years (Xin et al., 2018). The parameter n_{day} in the simple moving average method and the parameter k_1 in the time stepping method control the response of plant leaf allocation to environmental variation. The parameter n_{day} is set as 21 days and the parameter k_1 is calibrated as 0.080 day^{-1}.

This study compares four different modeling approaches, including the results simulated using both the SGPD model and the simple moving average method (hereinafter referred to as SGPD-SMA), using both the SGPD model and the time stepping scheme (hereinafter referred to as SGPD-TS), using both the GSI model and the simple moving average method (hereinafter referred to as GSI-SMA), and using both the GSI model and the time stepping scheme (hereinafter referred to as GSI-TS). The commonly used metrics, including the Pearson correlation coefficient (R), the coefficient of determination (R^2), the root-mean-square error (RMSE), and the mean bias error (MBE), are derived for model assessment and comparison.

3 Results

3.1 Site-scale modeling

Figure 1 shows an example for the simulated time series of LAI and GPP using data acquired at the US-WCr site in 2010 US-UMB in 2004. The LAI time series simulated using both the SGPD-SMA and SGPD-TS methods are consistent with that obtained from MODIS. The LAI simulated using both the GSI-SMA and GSI-TS methods could also capture the observed seasonal variation of LAI but the modeled phenophases obviously have a leading phase in spring and a lagging phase in autumn as compared with observations. For both the SGPD model and the GSI model, the results derived using the time stepping method are consistent with those derived using the simple moving average method, indicating that the time stepping method is an effective way to reflect the lagging responses of plant leaf allocation to environmental conditions. By substituting the time series of LAI derived from different modeling approaches into the MOD17 algorithm, all the simulated GPP time series could match the flux tower measurements. Daily fluctuation in the observed GPP time series is largely due to variation in solar radiation from day to day and is well captured by the models. The GPP modeled using both the GSI-SMA and GSI-TS methods have slight overestimates in the phenological transition periods like spring and autumn and match well with the flux tower observations in summer and winter.

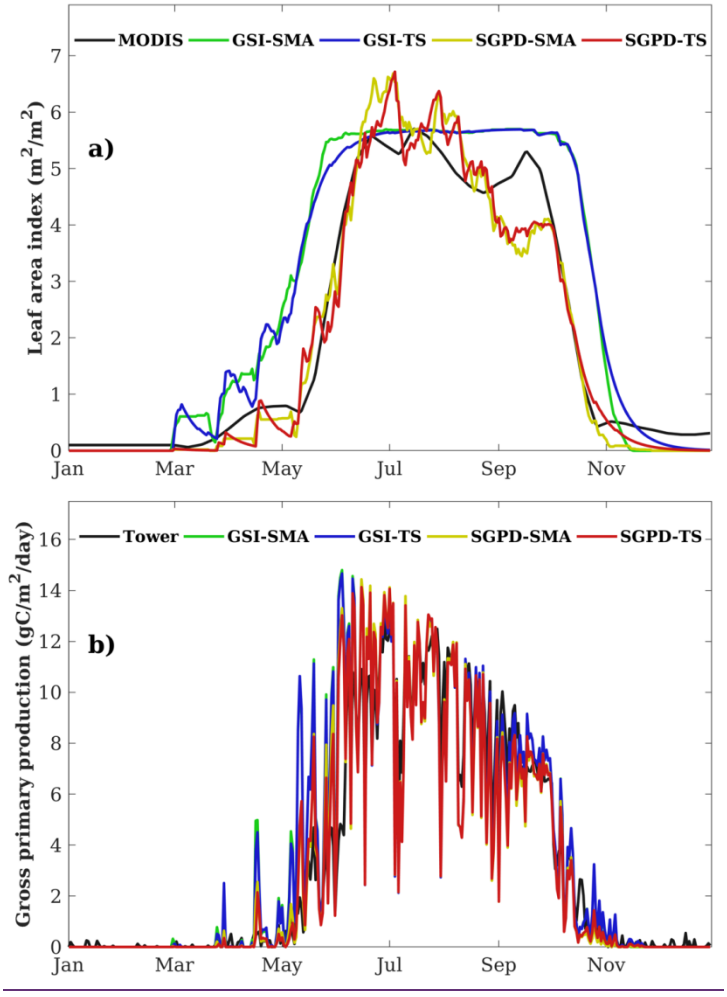

Figure 1: The modeled and measured daily time series of a) leaf area index and b) gross primary production are shown for the flux tower site of ~~US-WCr in 2010~~ US-UMB in 2004. The reference LAI time series in Figure 1a are derived from the MODIS data and the reference GPP time series in Figure 1b are obtained from the flux tower measurements.

Figure 2 shows the regression analysis between the modeled and satellite-derived LAI. Overall, the SGPD model outperforms the GSI model on modeling LAI. When evaluated against the MODIS LAI data, the SGPD-SMA and SGPD-TS models achieved the R^2 of 0.887 and 0.890, respectively, and the RMSE of 0.804 and 0.778 m^2/m^2, respectively, whereas the GSI-SMA and GSI-TS models achieved the R^2 of 0.746 and 0.759, respectively, and the RMSE of 1.356 and 1.303 m^2/m^2, respectively. Both the GSI-SMA and GSI-TS models simulate LAI reasonably in summer and winter but overestimate LAI in spring and autumn, and therefore, the strong correlations between the GSI-modeled and MODIS-derived LAI are largely due to the underlying seasonality of deciduous broadleaf forests. It is noteworthy that the time stepping method and the simple moving average method, despite having different mathematical expressions, generate nearly the same simulation

results. The R^2 values between the SGPD-TS model and the SGPD-SMA model and between the GSI-TS model and the GSI-SMA model are 0.989 and 0.994, respectively, and the regression lines are close to the lines of equity, indicating that the time stepping method is an alternative representation for the simple moving average method. ~~Because ecosystem processes are typically simulated at incremental time steps in terrestrial biosphere models, the time stepping method undoubtedly is more suitable than the simple moving average method for future uses in the land surface models.~~

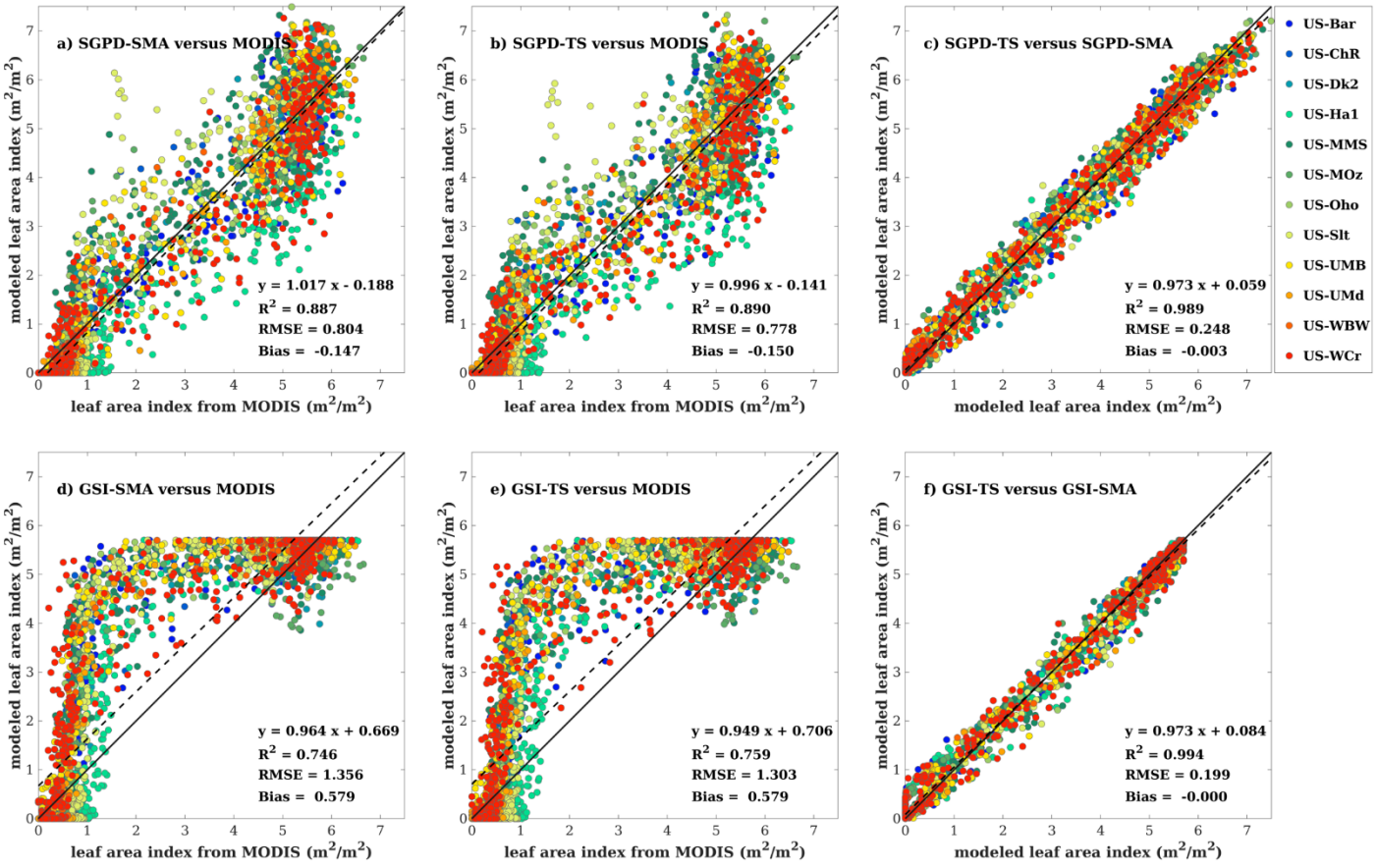

Figure 2: Scatter plots are shown for the comparisons a) between the SGPD-SMA LAI and the MODIS LAI, b) between the SGPD-TS LAI and the MODIS LAI, c) between the SGPD-TS LAI and the SGPD-SMA LAI, d) between the GSI-SMA LAI and the MODIS LAI, e) between the GSI-TS LAI and the MODIS LAI, and f) between the GSI-TS LAI and the GSI-SMA LAI on a weekly basis. All available site-year flux tower data were included in the analysis. The solid lines denote the 1:1 lines and the dashed lines denote the regression lines.

Table 2 lists the ~~statstical~~statistical metrics that illustrate the model performance on ~~preditingpredicting~~ the timing of different phenophases ~~are listed in~~. ~~The use of phenophases in model assessment eliminates the seasonality effects of the LAI times series.~~ As evaluated against satellite observations, the SGPD-SMA model could well retrieve the spring onset

dates when LAI reaches 50% seasonal amplitude and the obtained correlation coefficient is 0.718 with RMSE of 13.04 days. The SGPD-TS model performs comparable to the SGPD-SMA model and the resulted ~~corretion~~correlation coefficients are all significant expect for the dates that autumn LAI reaches 80% seasonal amplitudes. The SGPD-based models generally outperform~~s~~ the GSI-based models as the achieved correlation coefficients are higher and the RMSE are smaller for more than 10 days. Both the GSI-SMA and GSI-TS models predict spring onsets earlier than observations for more than 30 days and predict autumn ~~senenssence~~senescence later than observations for more than 20 days. By comparison, the SGPD-TS model predicts the dates that spring and autumn LAI reaches 50% seasonal amplitudes well with the MBE of only -2.56 and -2.86 days, respectively.

Table 2: The performance of the modeled timings of phenophases as evaluated against satellite observations. The timings of phenophases were derived based on dates at which the leaf area index reaches 20%, 50%, 80% of seasonal amplitude. Positive mean bias error (MBE) indicates that the modeled spring onsets are earlier than the observed ones and negative MBE indicates the opposite.

phenophases	SGPD-SMA			SGPD-TS			GSI-SMA			GSI-TS		
	R	RMSE (days)	MBE (days)	R	RMSE (days)	MBE (days)	R	RMSE (days)	MBE (days)	R	RMSE (days)	MBE (days)
Spring LAI 20%	0.790***	16.17	-10.85	0.824***	13.37	-8.34	0.763***	40.38	-38.30	0.770***	39.62	-37.58
Spring LAI 50%	0.718***	13.04	-1.97	0.691***	13.68	-2.56	0.653***	38.47	-34.92	0.657***	38.22	-34.63
Spring LAI 80%	0.432***	20.91	12.63	0.409***	21.19	12.41	0.560***	32.86	-28.00	0.565***	28.54	-23.55
Autumn LAI 80%	0.220	31.80	-25.56	0.164	27.90	-20.64	0.021	35.38	32.42	-0.004	35.23	32.27
Autumn LAI 50%	0.686***	9.80	-5.42	0.625***	9.48	-2.86	0.621***	24.20	23.07	0.616***	24.63	23.51
Autumn LAI 20%	0.703***	8.87	2.15	0.676***	10.91	6.37	0.689***	19.64	18.48	0.713***	22.93	22.00

The modeled and measured GPP are compared in Figure 3 to address the key question that whether the simulated LAI could be applied to model canopy GPP. Compared with the flux tower measurements, the results modeled using the SGPD-SMA, SGPD-TS, GSI-SMA, and GSI-TS LAI could achieve the R^2 values of 0.768, 0.773, 0.722, and 0.719, respectively, and the RMSE values of 2.273, 2.239, 2.577, 2.535 gC/m²/day, respectively. The modeled results using the GSI-based LAI have higher errors, in terms of both RMSE and MBE, than those using the SGPD-based LAI. The accuracies of the modeled GPP using the SGPD-based LAI are only slightly lower than to that using the MODIS-based LAI directly. The modeling results obtained based on the simple moving average method are nearly the same as those obtained based on the time stepping method. Given the high degrees of consistency between the simple moving average method and the time stepping method on modeling LAI, phenology, and GPP, only the results obtained using the time stepping method are shown and discussed in the regional studies as presented in the following section.

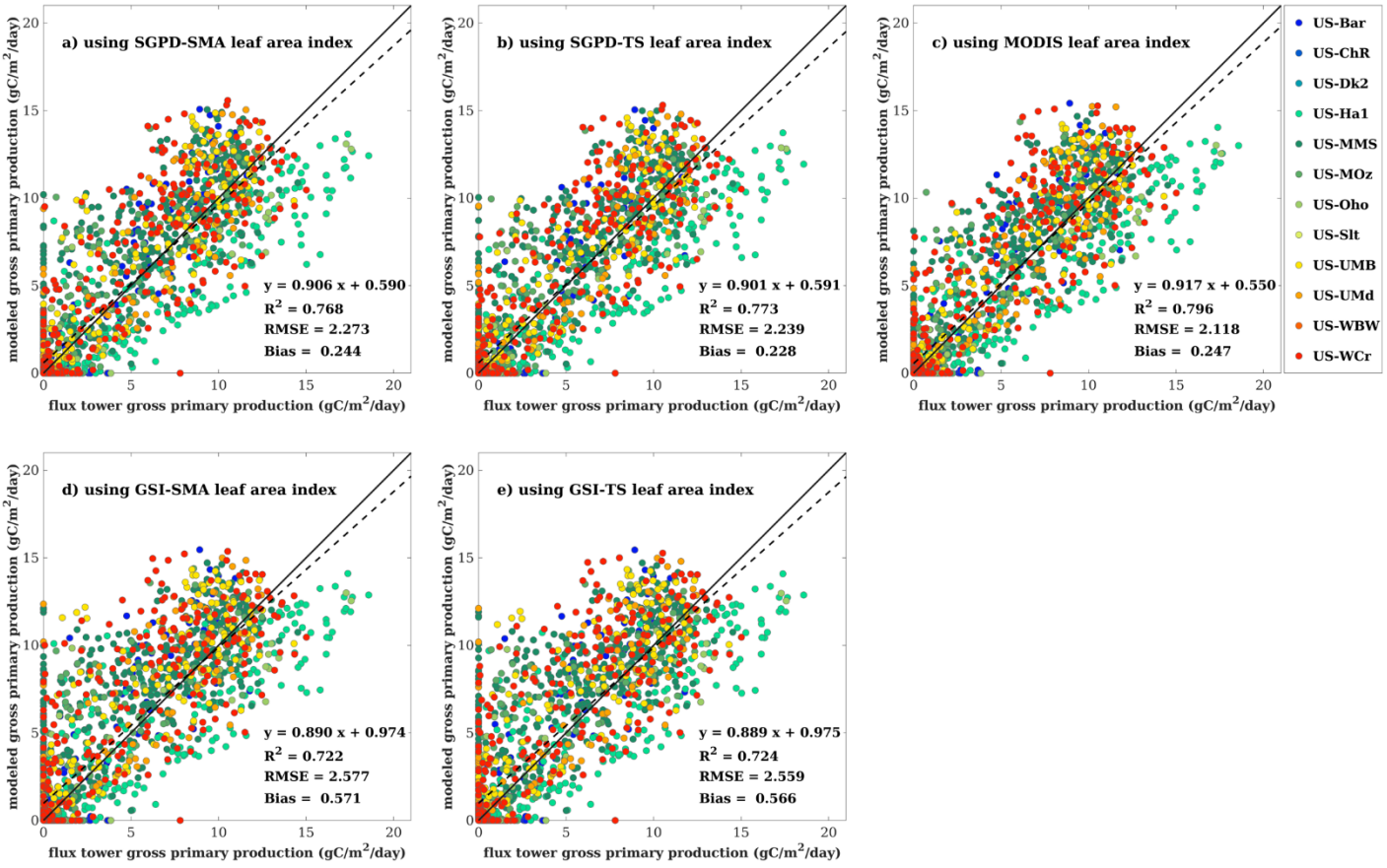

Figure 3: Scatter plots are shown for the comparisons a) between the GPP modeled using SGPD-SMA LAI and the flux tower GPP, b) between the GPP modeled using SGPD-TS LAI and the flux tower GPP, c) between the GPP modeled using MODIS LAI and the flux tower GPP, d) between the GPP modeled using GSI-SMA LAI and the flux tower GPP, and e) between the GPP modeled using GSI-TS LAI and the flux tower GPP on a weekly basis. All available site-year flux tower data were included in the analysis. All the modeled GPP were derived using the MOD17 algorithm. The solid lines denote the 1:1 lines and the dashed lines denote the regression lines.

3.2 Regional-scale modeling

Figure 4 shows the spatial extents of the 10-year (2001-2010) mean LAI and associated errors as derived from remote sensing data and model simulations. The SGPD-TS method could well capture the spatial pattern of the satellite-derived LAI, including the decreasing gradients from south to north and the decreases in mountain areas (Figure 4a and 4b). The 10-year mean LAI derived from the GSI-TS method (Figure 4c) also show a decreasing trend from south to north but the modeled LAI is much larger than the MODIS LAI. Because the GSI-TS method defines the maximum leaf area index for the growing season, the overestimation on the modeled 10-year mean LAI is primarily due to model overestimates in the spring and

autumn phenological transitions. As compared with the MODIS observations, RMSE and MBE obtained by the SGPD-TS method are much smaller than and distribute more evenly than those obtained by the GSI-TS method. RMSE for the GSI-TS LAI exhibit a decreasing north-south gradient, implying that the model accuracies are lower in southern areas lower than in northern areas. MBE for the GSI-TS model are greater than 0.5 m^2/m^2 for most areas. When comparing SGPD-TS LAI with MODIS LAI, RMSE are less than 0.5 m^2/m^2 and MBE are minor across the study region. The amplitudes of the error metrics in the regional-scale studies are consistent with those in the site-scale studies. Note that some studies applied the multi-year mean LAI as derived from the remote sensing data to simulate the land surface processes, the results obtained here indicate that the SGPD-TS method can be used alternatively to provide multi-year mean LAI time series via climate variables for land surface studies.

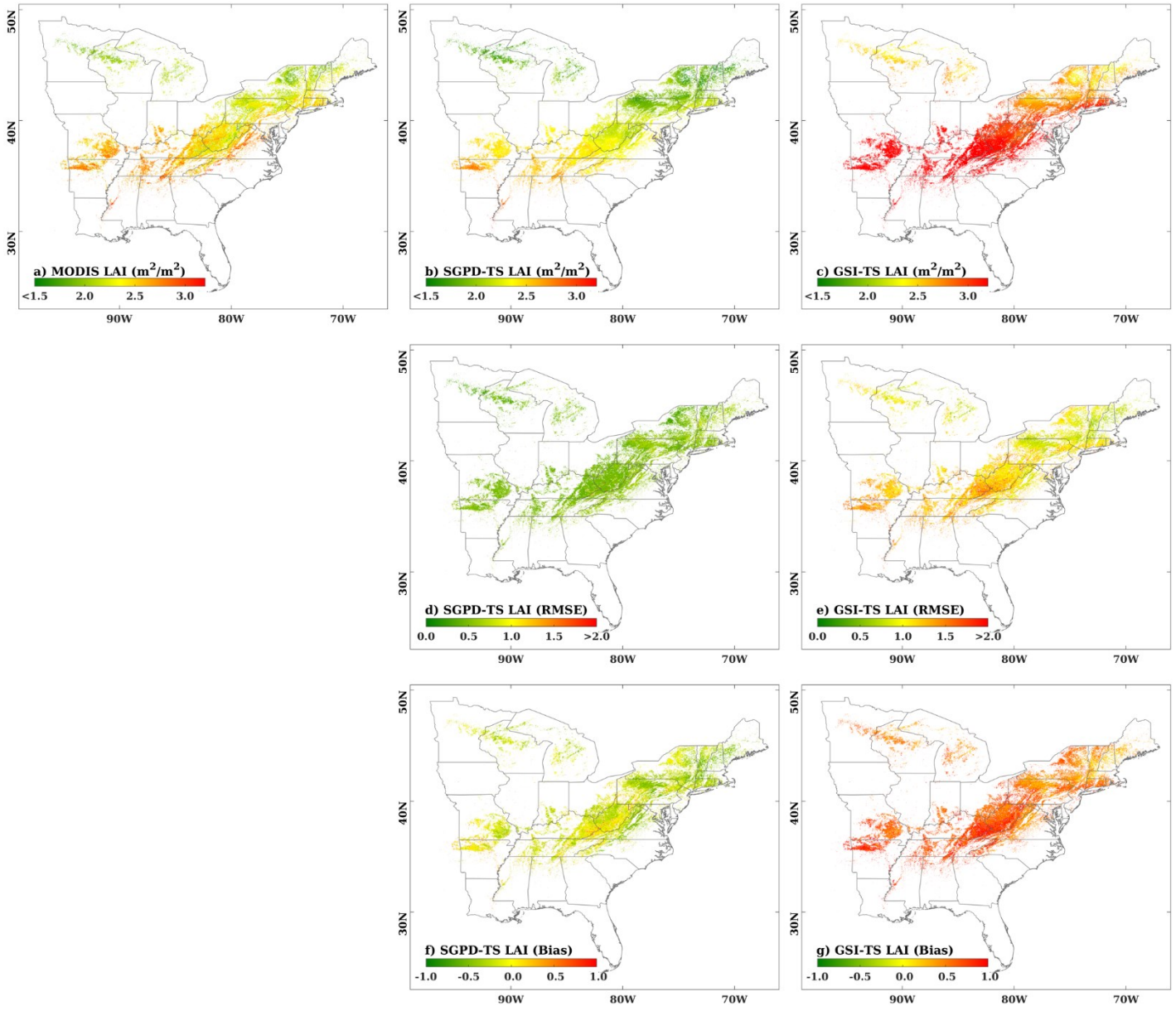

Figure 4: The spatial extents are shown for a) the 2001-2010 mean MODIS LAI, b) the 2001-2010 mean SGPD-TS LAI, c) the 2001-2010 mean GSI-TS LAI, d) RMSE between SGPD-TS LAI and MODIS LAI, e) RMSE between GSI-TS LAI and MODIS LAI, f) MBE between SGPD-TS LAI and MODIS LAI, and g) MBE between GSI-TS LAI and MODIS LAI across eastern United States. The units for both RMSE and MBE are m² (leaf area) per m² (ground area).

The spatial extents for the 10-year mean phenological metrics including the start of the season (SOS), the end of the season (EOS), and the growing season length (GSL) are shown in Figure 5. The SGPD-TS method predicts lower SOS (i.e., earlier spring onset), higher EOS (i.e., later autumn senescence), and longer GSL in southern areas than in northern areas. The

spatial distributions of all phenological metrics derived using SGPD-TS LAI agree well with those derived using MODIS LAI. From the statistical analysis as shown in the subplots, the phenological metrics derived from the SGPD-TS method could achieve the correlation coefficient values of 0.879, 0.552, and 0.844, the RMSE values of 8.13, 7.54, and 13.73 days, and the MBE values of 0.71, -2.82, and -3.54 days, for SOS, EOS, and GSL, respectively, as compared to those derived from the MODIS data. Although the spatial distributions of the phenological metrics derived from the GSI-TS method match those derived from the satellite observations, the modeled results have considerable biases, where the RMSE values are 38.05, 14.37, and 51.58 days, and the MBE values are -36.33, 12.91, and 49.23 days, for SOS, EOS, and GSL, respectively. Consistent with the site-scale studies, the GSI-TS method predicts spring onset much earlier and autumn senescence later than the satellite-derived data, resulting in large overestimation of the growing season length. ~~Despite having limited model accuracies as compared with observations, the GSI-TS method here performs comparable to or even better than the other phenology models in similar modeling studies.~~

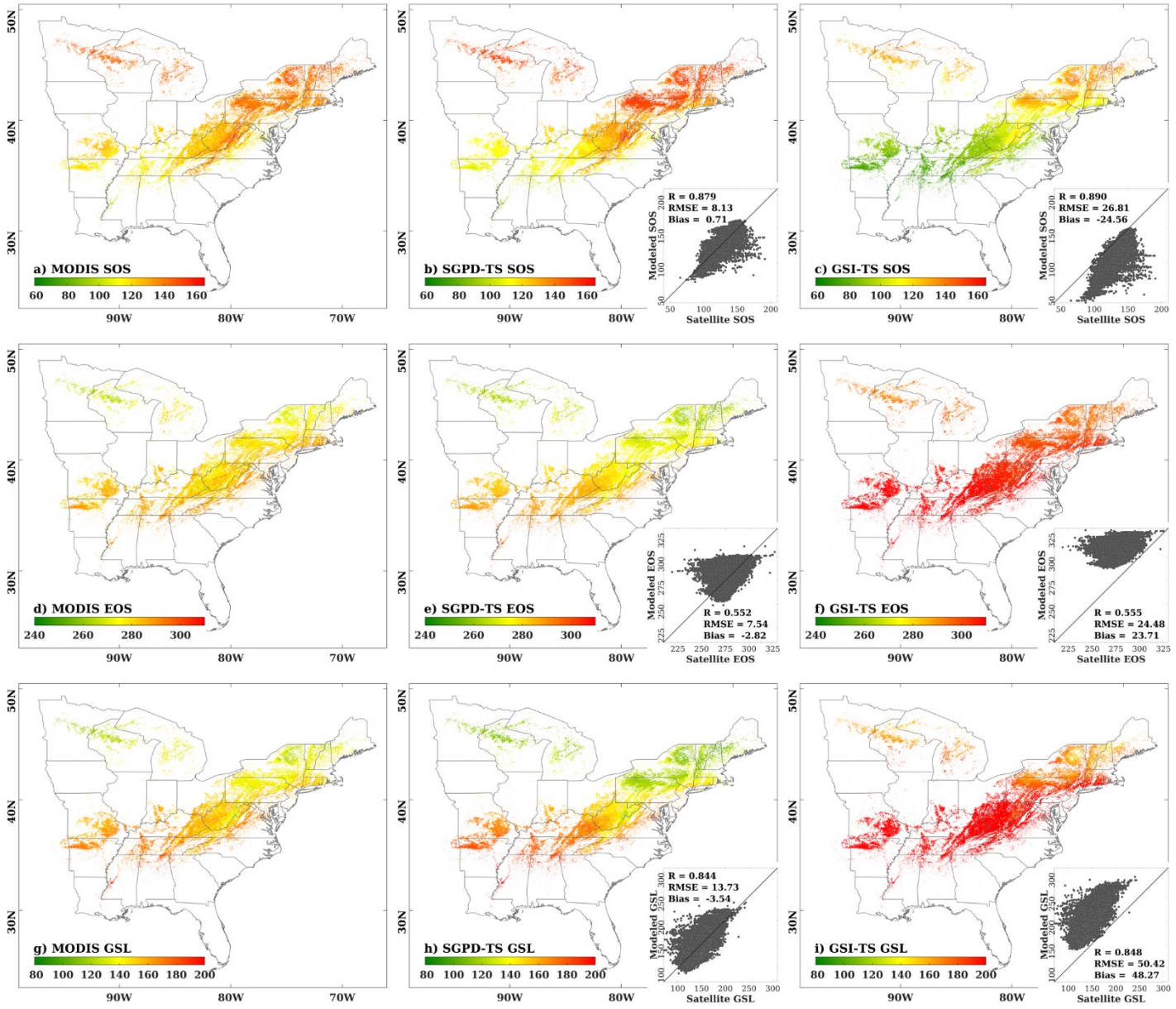

Figure 5: The spatial extents are shown for a) the start of the season (SOS) derived from MODIS LAI, b) SOS derived from SGPD-TS LAI, c) SOS derived from GSI-TS LAI, d) the end of the season (EOS) derived from MODIS LAI, e) EOS derived from SGPD-TS LAI, f) EOS derived from GSI-TS LAI, g) the growing season length (GSL) derived from MODIS LAI, h) GSL derived from SGPD-TS LAI, and i) GSL derived from GSI-TS LAI using the 10-year (2001-2010) mean data across eastern United States. The embedded subplots show the comparisons between modeled and MODIS-derived phenological metrics for SOS, EOS, and GSL, respectively.

Figure 6 displays the multi-year phenology anomalies that are spatially averaged for deciduous broadleaf forest across eastern United States. The use of phenology anomalies relative to the 2001-2010 average instead of absolute values makes the results directly comparable. The SGPD-TS method could capture the interannual variation of vegetation phenology retrieved from the remote sensing data. When comparing the SGPD-TS method with the MODIS (2001-2016) data, the correlation coefficients are 0.896 ($p<0.001$), 0.650 ($p=0.006$), and 0.817 ($p<0.001$), for SOS, EOS, and GSL, respectively. When comparing the SGPD-TS method with the GLASS (1982-2014) data, as derived from and the correlation coefficients are 0.554 ($p=0.001$), 0.717 ($p<0.001$), 0.637 ($p<0.001$), for SOS, EOS, and GSL, respectively. The SGPD-TS method outperforms the GSI-TS method on capturing the long-term trends of vegetation phenophases, as the correlation coefficients obtained using the GSI-TS method are lower and sometimes insignificant. Yearly fluctuation in EOS derived using the GSI-TS method is smaller than those derived from both the SGPD-TS method and the satellite data. The SOS and EOS derived from the GLASS data have much larger variation in 1982-2000 than in 2001-2010, suggesting that the use of the AVHRR and MODIS data in the GLASS dataset could contribute uncertainties in the satellite-derived phenological metrics. Both Figure 5 and 6 indicate that the SGPD-TS method is reliable on capturing the spatiotemporal patterns of regional vegetation phenophases.

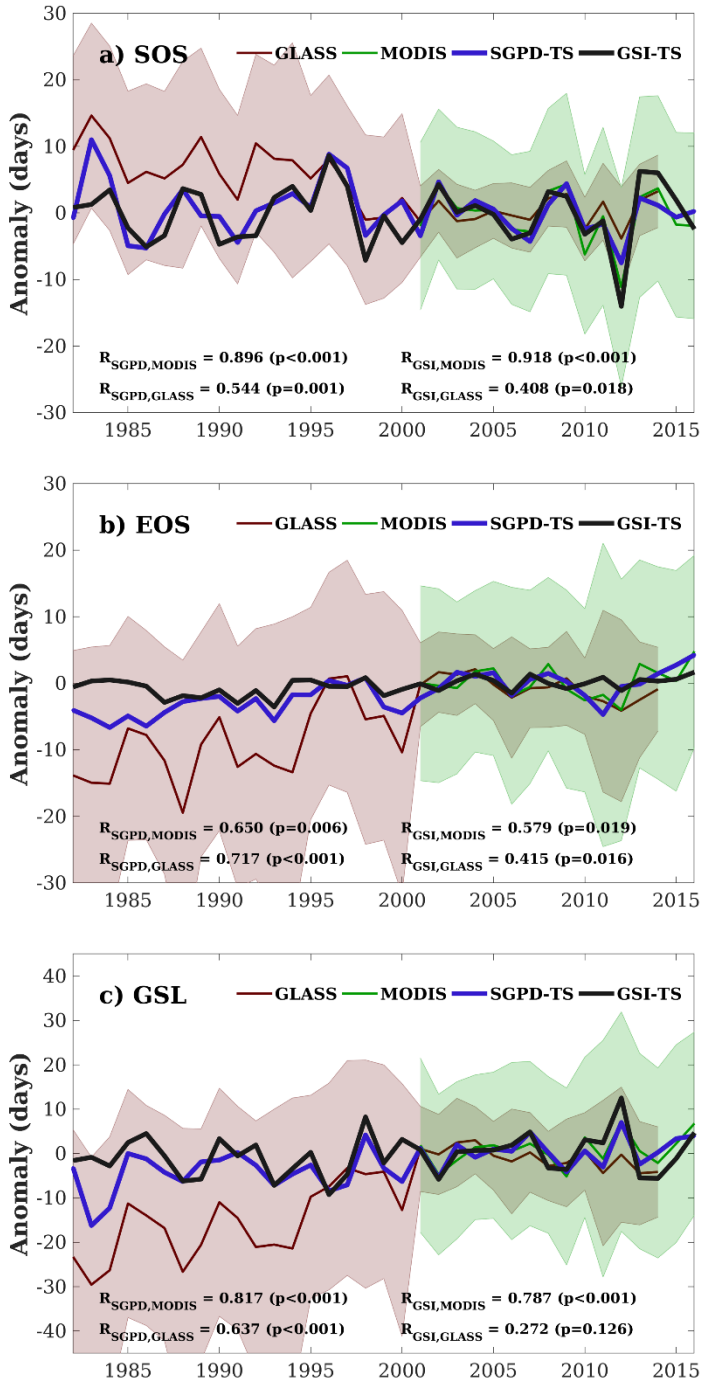

Figure 6: The spatially-averaged phenology anomalies relative to the 2001-2010 average are shown for a) the start of the season (SOS), b) the end of the season (EOS), and c) the growing season length (GSL). SOS and EOS are derived as the date that LAI first and last reaches 50% of the seasonal amplitudes and GSL is derived as the difference between EOS and SOS.

Figure 7 compares the simulated ~~c~~ GPP using the MOD17 algorithm and LAI derived from different approaches. The 10-year average annual GPP obtained using SGPD-TS LAI has a similar spatial pattern with that obtained using MODIS LAI and ~~apparently~~ has lower values than that obtained using GSI-TS LAI. Taking the GPP simulated using MODIS LAI as reference, the results simulated using SGPD-TS LAI achieve the correlation coefficient of 0.898 with RMSE of 78.78 gC/m²/year and MBE of 12.22 gC/m²/year, whereas the results simulated using GSI-TS LAI achieve the correlation coefficient of 0.898 with RMSE of 173.45 gC/m²/year and MBE of 153.43 gC/m²/year. Although the obtained correlation coefficients are close, the SGPD-TS method results in the regression lines closer to the 1:1 lines with smaller bias errors than the GSI-TS method. The zonally average profiles of the 2001-2010 average annual GPP as shown in Figure 7d suggest that the results obtained from the SGPD-TS method are close to those obtained using MODIS LAI, whereas the results obtained from the GSI-TS method have positive biases of approximately 120 - 180 gC/m2/year (roughly 10 - 15%) across latitudes. Note that the MOD17 algorithm has positive MBE of 0.247 gC/m2/day and 0.571 gC/m2/day when using ~~MODIS~~ SGPD-TS LAI and GSI-TS LAI, respectively, as model input data in the site-scale study. The differences in MBE between the two modeling methods are 0.324 gC/m2/day (or 118.26 gC/m2/year in equivalence) for the site-scale studies, which are consistent with the regional-scale studies.

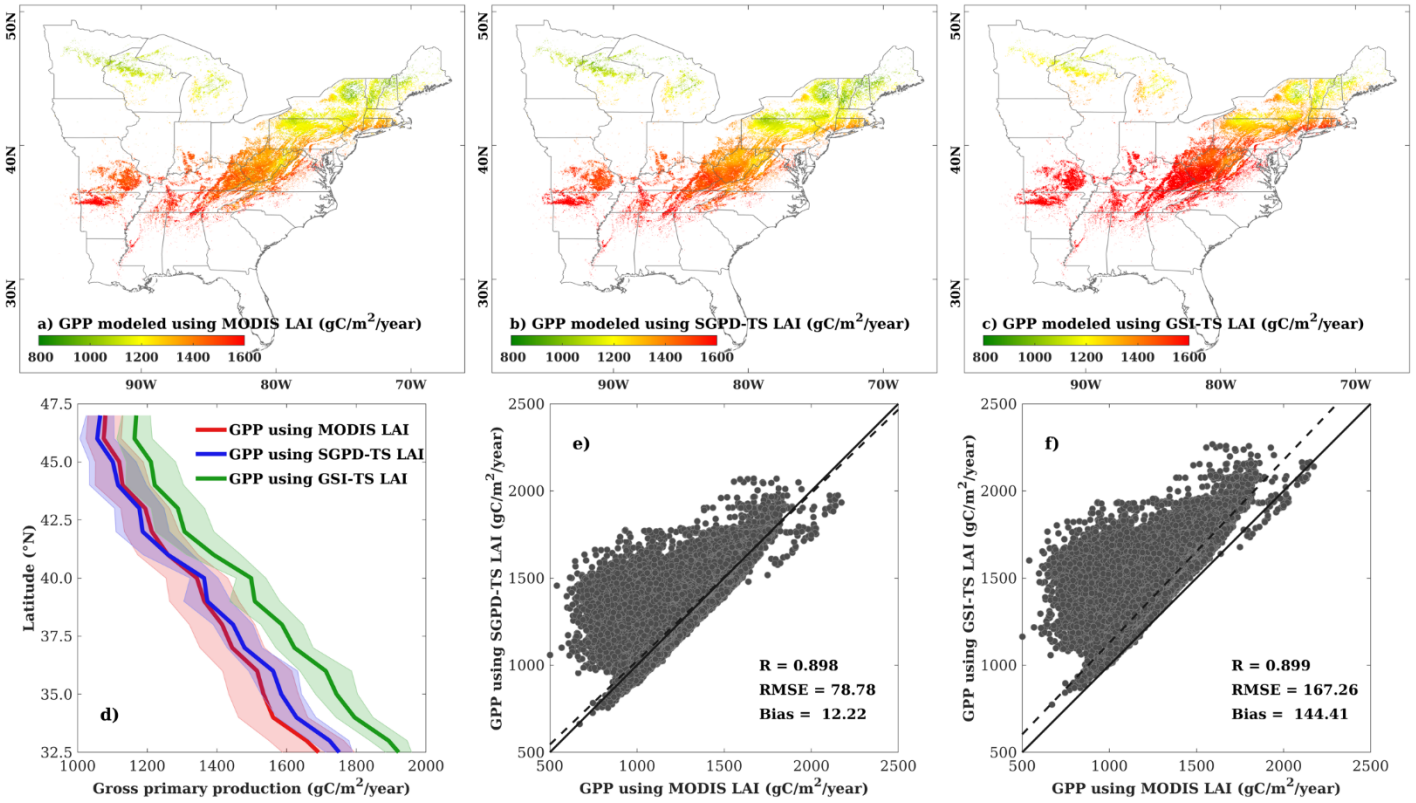

Figure 7: Comparisons are shown for a) the spatial extent of annual GPP modeled using MODIS LAI, b) the spatial extent of annual GPP modeled using SGPD-TS LAI, c) the spatial extent of annual GPP modeled using GSI-TS LAI, d) the zonally averaged profiles of annual gross primary production modeled using LAI derived from different approaches, e) the regression between GPP modeled using SGPD-TS LAI and MODIS LAI, and f) the regression between GPP modeled using GSI-TS LAI and MODIS LAI. The simulated daily GPP were first summed for each individual year and were then averaged across years to derive the 2001-2010 average annual GPP as shown in Figure 7a, 7b, and 7c. The shaded areas in Figure 7d mark the range of the standard deviation. All pixels of deciduous broadleaf forest across eastern United States are included in analysis in Figure 7e and 7f.

4 Discussion

Here we provide a solution that bridges the canopy photosynthesis model and the leaf dynamics model~~, which overcomes the weakness that existing studies developed the plant phenology model independent of the canopy photosynthesis model~~. The developed method first proposes a linear function between the canopy photosynthetic capacity and the steady state LAI so as to complement the canopy photosynthesis model and then applies a simple restricted growth model to account for the lagged responses of plant leaf allocation to natural environment. In essence, the developed method, although having a simple form, has synthesized the impacts of various climate factors on leaf dynamics because any climate variable that influences vegetation photosynthesis would affect the process of plant leaf allocation in the models as well. Consistent with field observations, the simulated LAI increases as the environmental conditions turn favorable for photosynthetic activities such

as increases in photoperiod and temperature. ~~It is worth noting that our modeling approach is essentially based on an ecological assumption that plants have evolved strategies to optimize leaf distribution according to the environmental carrying capacity for maximizing photosynthetic carbon gain. The assumption undoubtedly requires observational supports from extensive experiments, preferably laboratory controlling experiments, on plant physiology and phenology in future studies.~~

Figure 8 further illustrate the relationship between mean LAI and different variables on a monthly basis. All data were averaged to the monthly time scale such that canopy LAI can be considered as nearly the steady state. On the monthly basis, mean LAI has a strong near-linear relationship with mean GPP (R^2=0.888) and the slope for the regression without intercept is 0.580, the same as we used in the model simulation. On the monthly basis, mean LAI is strongly correlated with mean temperature (R^2=0.799), indicating that temperature is the dominate factor that determines vegetation phenology. Factors like vapor pressure deficit and photoperiod also have positive relationships with mean LAI on the monthly basis. Figure 8 suggests that the processes of leaf phenology and photosynthetic phenology for deciduous broadleaf forest are closely related. Our modeling approach that links canopy GPP with LAI reflects the empirical positive relationship found in Figure 8a.

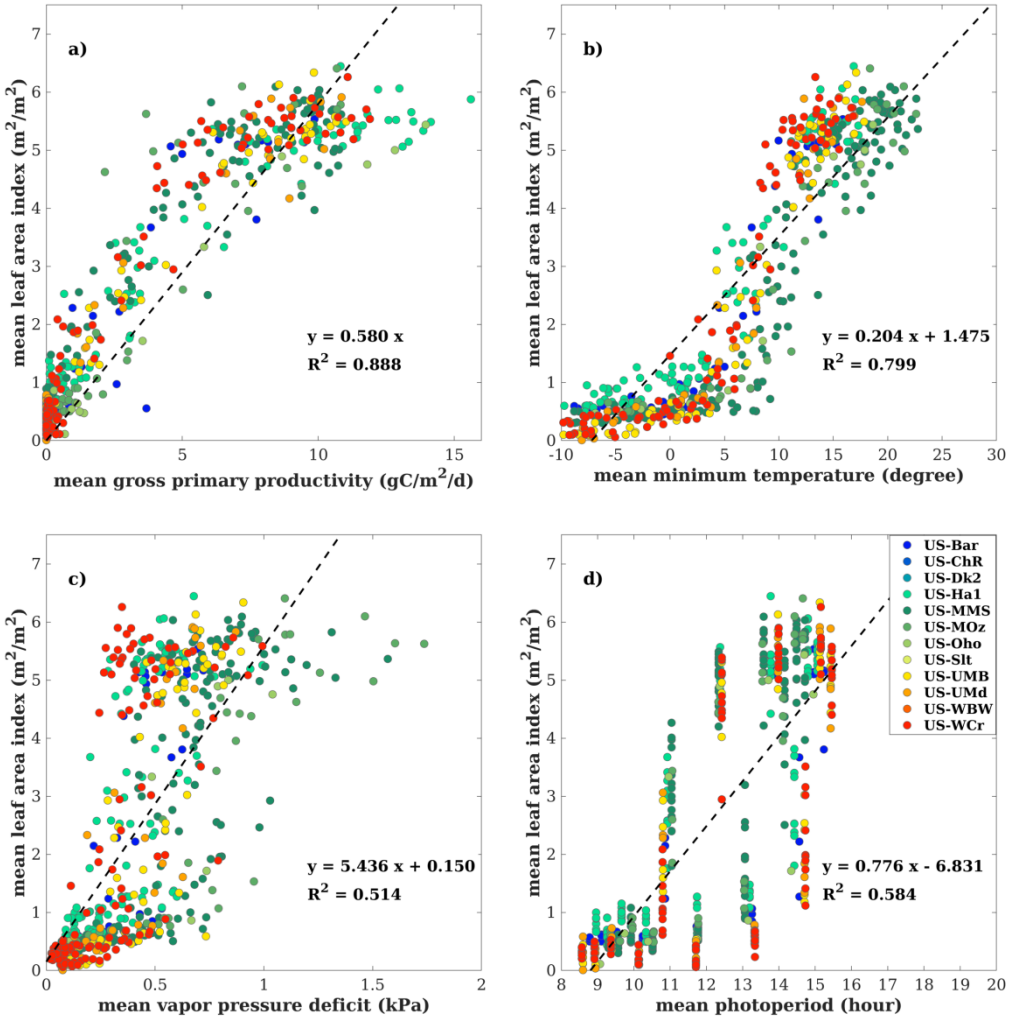

Figure 8: Scatter plots are shown for the relationship a) between mean leaf area index and mean gross primary production, b) between mean leaf area index and mean temperature, c) between mean leaf area index and mean vapor pressure deficit, and d) mean leaf area index and mean photoperiod on a monthly basis. All available site-year flux tower data were included in the analysis. All data were averaged to the monthly time scale for analysis. The dashed lines denote the regression lines. Figure 8a uses the regression without intercept.

The performance of our developed method is largely dependent on the canopy photosynthesis model used. In our previous studies, we developed a process-based canopy photosynthesis model that synthesizes sub-models such as canopy radiative transfer, leaf transpiration, leaf stomatal conductance, leaf photosynthesis, and soil evaporation and applied it for modeling the LAI time series. When applying the simple moving average method, implementing the process-based model in Xin et al. (2018) achieved higher accuracies than implementing the MOD17 algorithm on modeling canopy GPP and LAI as reflected by higher R^2 and lower errors. The MOD17 algorithm only assumes the monotonic relationship between air temperature and

photosynthesis and between vapor pressure deficit and photosynthesis. It also does not account for the impacts of CO_2 on photosynthesis. The use of the MOD17 algorithm in this study thus has limitations in the model structure. It implies that the LAI modeling in our developed method likely benefits from improvements on the canopy photosynthesis model. This study chooses the MOD17 algorithm instead of the sophisticated process-based model because the MOD17 algorithm is well parameterized across biomes and requires quite limited model inputs of climate variables. Successful implementation with the MOD17 algorithm allows for extending the developed method to applications across biomes at regional to global scales.

Land surface models that predict vegetation GPP require either satellite-derived LAI input data or the phenology sub-model. The main idea for this study is to improve the phenology modeling by providing time series of LAI simulated using climate variables, and hence enables to simulate GPP forced only by climate variables. Because we implement the MOD17 algorithm instead of the sophisticated process-based model for the purpose of simplicity, one should not expect that GPP simulated based on the model-simulated LAI could be more accurate than GPP simulated based on the satellite-derived LAI.

The time stepping scheme developed here is also an improvement over the simple moving average method as used in our previous studies. The results obtained using the time stepping method are consistent with the simple moving average method at the site scale and show to be reasonable at the regional scale. Compared to the simple moving average method, the time stepping method could fit seamlessly into the land surface models that operate at incremental time steps such as the Community Land Model and the Common Land Model (Dai et al., 2003). Because the state-of-the-art land surface models all include the canopy photosynthesis sub-model, the developed method can then be easily embedded into these land surface models as an alternative phenology model. Compared to the simple light use efficiency model like the MOD17 algorithm, implementation of the developed time-stepping scheme in the land surface models relies on supercomputing for global applications. To better understand the performance of the developed method, one study is now undertaken to implement the developed method with the Common Land Model for simulating multi-decadal LAI and GPP for global biomes ~~via~~ forced only by climate variables.

Applying the developed method to other biomes and other regions still has issues to be solved appropriately. The time stepping method uses the parameter k_l to account for the time lags of leaf allocation in response to environmental changes. For the deciduous broadleaf forests, a biome with strong seasonality, the developed scheme achieved reasonable results with appropriate parameterization. Short vegetation like grasslands tends to respond much quickly to abrupt environment changes like precipitation and tropical ecosystems have strong resilience to short-term environmental variation (Levine et al., 2016; Shen et al., 2011). Another issue is to find the appropriate values of m for different biomes. One way to determine the values of m is to find the regression slope between leaf area index and gross primary production on a monthly basis. Model parameterization however still requires broad tests. These understandings from the observational studies imply that biomes have varied response speeds to the environment and proper model calibration and assessment are required for the developed

method. Using the observation data from remote sensing alone is inadequate for model development as satellite-derived LAI could have large uncertainties for some specific biomes other than deciduous broadleaf forests. Fortunately, global flux tower network and regional phenology observation networks are now established and offer abundant data for comprehensive model assessment.

5 Conclusions

~~Robust t~~Terrestrial biosphere models ~~is~~ provide a basic tool for understanding the interactions between the land surface and the atmosphere. To provide a complete solution to the simulation of plant leaf dynamics and canopy photosynthesis, this study establishes a linear relationship between the steady state leaf area index and the corresponding canopy photosynthetic capacity ~~based on the idea that plants optimize leaf biomass allocation according to the environmental carrying capacity for maximizing photosynthetic carbon gain~~. The proposed leaf allocation function complements the canopy photosynthesis model of the MOD17 algorithm to form simultaneous equations that can be solved ~~iteratively~~ using the numerical approach. To account for the time lagging of plant leaf allocation in response to climate variation, a time stepping scheme based on a simple restricted growth model is applied to the solved steady state leaf area index to obtain time series of leaf area index. The developed method could perform reasonably well on simulating leaf area index, phenology, and gross primary production for deciduous broadleaf forests across eastern United States over years as found in both the site-scale and regional-scale modeling studies. Compared to the simple moving average method, the time stepping scheme developed here is consistent with and can be easily embedded into the state-of-the-art land surface models that typically operate at incremental time steps. The developed method allows for simulating leaf area index and gross primary production simultaneously and provides a much simplified and improved version of our previous model as a basis for global applications in future studies.

Author contributions

Qinchuan Xin designed the experiments and performed the simulations. All authors interpreted the results. Qinchuan Xin wrote the manuscript with contributions from all coauthors. The authors declare that they have no conflict of interest.

Acknowledgments

We thank the researchers and investigators who are involved in collecting and sharing the AmeriFlux dataset. This research is supported by National Key R&D Program of China (grant nos. 2017YFA0604302 and 2017YFA0604402) and National Natural Science Foundation of China (grant no. 41875122). We also thank anonymous reviewers for their constructive comments.

References

Akaike, H.: Fitting autoregressive models for prediction, Annals of the institute of Statistical Mathematics, 21, 243-247, 1969.

Allen, R. G., Pereira, L. S., Raes, D., and Smith, M.: Crop evapotranspiration-Guidelines for computing crop water requirements-FAO Irrigation and drainage paper 56, FAO, Rome, 300, 6541, 1998.

Beer, C., Reichstein, M., Tomelleri, E., Ciais, P., Jung, M., Carvalhais, N., Roedenbeck, C., Arain, M. A., Baldocchi, D., Bonan, G. B., Bondeau, A., Cescatti, A., Lasslop, G., Lindroth, A., Lomas, M., Luyssaert, S., Margolis, H., Oleson, K. W., Roupsard, O., Veenendaal, E., Viovy, N., Williams, C., Woodward, F. I., and Papale, D.: Terrestrial Gross Carbon Dioxide Uptake: Global Distribution and Covariation with Climate, Science, 329, 834-838, 2010.

Bonan, G. B.: Ecological climatology: concepts and applications, Cambridge University Press, 2002.

Bonan, G. B.: Forests and climate change: forcings, feedbacks, and the climate benefits of forests, science, 320, 1444-1449, 2008.

Broxton, P. D., Zeng, X., Sulla-Menashe, D., and Troch, P. A.: A global land cover climatology using MODIS data, Journal of Applied Meteorology and Climatology, 53, 1593-1605, 2014.

Chuine, I., Cour, P., and Rousseau, D. D.: Selecting models to predict the timing of flowering of temperate trees: implications for tree phenology modelling, Plant Cell and Environment, 22, 1-13, 1999.

Clark, K. L., Skowronski, N., Gallagher, M., Renninger, H., and Schäfer, K.: Effects of invasive insects and fire on forest energy exchange and evapotranspiration in the New Jersey pinelands, Agricultural and Forest Meteorology, 166, 50-61, 2012.

Dai, Y., Zeng, X., Dickinson, R. E., Baker, I., Bonan, G. B., Bosilovich, M. G., Denning, A. S., Dirmeyer, P. A., Houser, P. R., and Niu, G.: The common land model, Bulletin of the American Meteorological Society, 84, 1013-1023, 2003.

De Réaumur, R. A. F.: Observations du thermometer, faites à Paris pendant l'année 1735, comparées avec celles qui ont été faites sous la ligne, à l'Isle de France, à Alger et en quelques-unes de nos isles de l'Amérique, Mémoires de l'Académie des Sciences, 1735. 545-584, 1735.

Desai, A. R., Noormets, A., Bolstad, P. V., Chen, J., Cook, B. D., Davis, K. J., Euskirchen, E. S., Gough, C., Martin, J. G., and Ricciuto, D. M.: Influence of vegetation and seasonal forcing on carbon dioxide fluxes across the Upper Midwest, USA: Implications for regional scaling, agricultural and forest meteorology, 148, 288-308, 2008.

Ding, R., Kang, S., Du, T., Hao, X., and Zhang, Y.: Scaling Up Stomatal Conductance from Leaf to Canopy Using a Dual-Leaf Model for Estimating Crop Evapotranspiration, PloS one, 9, e95584, 2014.

Dragoni, D., Schmid, H. P., Wayson, C. A., Potter, H., Grimmond, C. S. B., and Randolph, J. C.: Evidence of increased net ecosystem productivity associated with a longer vegetated season in a deciduous forest in south-central Indiana, USA, Global Change Biology, 17, 886-897, 2011.

Eagleson, P. S.: Ecohydrology: Darwinian expression of vegetation form and function, Cambridge University Press, 2005.

Givnish, T. J.: On the Economy of Plant Form and Function: Proceedings of the Sixth Maria Moors Cabot Symposium, Evolutionary Constraints on Primary Productivity, Adaptive Patterns of Energy Capture in Plants, Harvard Forest, August 1983, Cambridge University Press, 1986.

Gough, C. M., Hardiman, B. S., Nave, L. E., Bohrer, G., Maurer, K. D., Vogel, C. S., Nadelhoffer, K. J., and Curtis, P. S.: Sustained carbon uptake and storage following moderate disturbance in a Great Lakes forest, Ecological Applications, 23, 1202-1215, 2013.

Gu, L., Meyers, T., Pallardy, S. G., Hanson, P. J., Yang, B., Heuer, M., Hosman, K. P., Riggs, J. S., Sluss, D., and Wullschleger, S. D.: Direct and indirect effects of atmospheric conditions and soil moisture on surface energy partitioning revealed by a prolonged drought at a temperate forest site, Journal of Geophysical Research: Atmospheres (1984–2012), 111, 2006.

He, M., Ju, W., Zhou, Y., Chen, J., He, H., Wang, S., Wang, H., Guan, D., Yan, J., Li, Y., Hao, Y., and Zhao, F.: Development of a two-leaf light use efficiency model for improving the calculation of terrestrial gross primary productivity, Agricultural and Forest Meteorology, 173, 28-39, 2013.

Hollinger, D. Y., Ollinger, S., Richardson, A., Meyers, T., Dail, D., Martin, M., Scott, N., Arkebauer, T., Baldocchi, D., and Clark, K.: Albedo estimates for land surface models and support for a new paradigm based on foliage nitrogen concentration, Global Change Biology, 16, 696-710, 2010.

Hufkens, K., Basler, D., Milliman, T., Melaas, E. K., and Richardson, A. D.: An integrated phenology modelling framework in R, Methods in Ecology and Evolution, 9, 1276-1285, 2018.

Jenkins, J., Richardson, A. D., Braswell, B., Ollinger, S. V., Hollinger, D. Y., and Smith, M.-L.: Refining light-use efficiency calculations for a deciduous forest canopy using simultaneous tower-based carbon flux and radiometric measurements, Agricultural and Forest Meteorology, 143, 64-79, 2007.

Jolly, W. M., Nemani, R., and Running, S. W.: A generalized, bioclimatic index to predict foliar phenology in response to climate, Global Change Biology, 11, 619-632, 2005.

Levine, N. M., Zhang, K., Longo, M., Baccini, A., Phillips, O. L., Lewis, S. L., Alvarez-Dávila, E., de Andrade, A. C. S., Brienen, R. J., and Erwin, T. L.: Ecosystem heterogeneity determines the ecological resilience of the Amazon to climate change, Proceedings of the National Academy of Sciences, 113, 793-797, 2016.

Li, W., Guo, Q., Tao, S., and Su, Y.: VBRT: A novel voxel-based radiative transfer model for heterogeneous three-dimensional forest scenes, Remote Sensing of Environment, 206, 318-335, 2018.

Liu, J., Chen, J., Cihlar, J., and Park, W.: A process-based boreal ecosystem productivity simulator using remote sensing inputs, Remote sensing of environment, 62, 158-175, 1997.

Liu, Q., Fu, Y. H., Liu, Y., Janssens, I. A., and Piao, S.: Simulating the onset of spring vegetation growth across the Northern Hemisphere, Global change biology, 24, 1342-1356, 2018.

Melaas, E. K., Friedl, M. A., and Richardson, A. D.: Multiscale modeling of spring phenology across Deciduous Forests in the Eastern United States, Glob. Change Biol., 22, 792-805, 2016.

Melaas, E. K., Richardson, A. D., Friedl, M. A., Dragoni, D., Gough, C. M., Herbst, M., Montagnani, L., and Moors, E.: Using FLUXNET data to improve models of springtime vegetation activity onset in forest ecosystems, Agricultural and Forest Meteorology, 171, 46-56, 2013.

Miller, G. R., Baldocchi, D. D., Law, B. E., and Meyers, T.: An analysis of soil moisture dynamics using multi-year data from a network of micrometeorological observation sites, Advances in Water Resources, 30, 1065-1081, 2007.

Myneni, R. B., Hoffman, S., Knyazikhin, Y., Privette, J. L., Glassy, J., Tian, Y., Wang, Y., Song, X., Zhang, Y., Smith, G. R., Lotsch, A., Friedl, M., Morisette, J. T., Votava, P., Nemani, R. R., and Running, S. W.: Global products of vegetation leaf area and fraction absorbed PAR from year one of MODIS data, Remote Sensing of Environment, 83, 214-231, 2002.

Ni-Meister, W., Yang, W., and Kiang, N. Y.: A clumped-foliage canopy radiative transfer model for a global dynamic terrestrial ecosystem model. I: Theory, Agricultural and forest meteorology, 150, 881-894, 2010.

Oishi, A. C., Oren, R., and Stoy, P. C.: Estimating components of forest evapotranspiration: a footprint approach for scaling sap flux measurements, Agricultural and Forest Meteorology, 148, 1719-1732, 2008.

Oleson, K., Lawrence, D., Bonan, G., Drewniak, B., Huang, M., Koven, C., Levis, S., Li, F., Riley, W., and Subin, Z.: Technical Description of version 4.5 of the Community Land Model (CLM), NCAR, National Center for Atmospheric Research (NCAR) Boulder, Colorado, 2013. 2013.

Polgar, C. A. and Primack, R. B.: Leaf-out phenology of temperate woody plants: from trees to ecosystems, New Phytologist, 191, 926-941, 2011.

Potter, C. S., Randerson, J. T., Field, C. B., Matson, P. A., Vitousek, P. M., Mooney, H. A., and Klooster, S. A.: Terrestrial ecosystem production: a process model based on global satellite and surface data, Global Biogeochemical Cycles, 7, 811-841, 1993.

Richardson, A. D., Anderson, R. S., Arain, M. A., Barr, A. G., Bohrer, G., Chen, G. S., Chen, J. M., Ciais, P., Davis, K. J., Desai, A. R., Dietze, M. C., Dragoni, D., Garrity, S. R., Gough, C. M., Grant, R., Hollinger, D. Y., Margolis, H. A., McCaughey, H., Migliavacca, M., Monson, R. K., Munger, J. W., Poulter, B., Raczka, B. M., Ricciuto, D. M., Sahoo, A. K., Schaefer, K., Tian, H. Q., Vargas, R., Verbeeck, H., Xiao, J. F., and Xue, Y. K.: Terrestrial biosphere models need better representation of vegetation phenology: results from the North American Carbon Program Site Synthesis, Global Change Biology, 18, 566-584, 2012.

Running, S. W., Nemani, R. R., Heinsch, F. A., Zhao, M. S., Reeves, M., and Hashimoto, H.: A continuous satellite-derived measure of global terrestrial primary production, Bioscience, 54, 547-560, 2004.

Running, S. W. and Zhao, M.: Daily GPP and annual NPP (MOD17A2/A3) products NASA Earth Observing System MODIS land algorithm, MOD17 User's Guide, 2015. 2015.

Ryu, Y., Baldocchi, D. D., Kobayashi, H., Ingen, C., Li, J., Black, T. A., Beringer, J., Gorsel, E., Knohl, A., and Law, B. E.: Integration of MODIS land and atmosphere products with a coupled-process model to estimate gross primary productivity and evapotranspiration from 1 km to global scales, Global Biogeochemical Cycles, 25, GB4017, 2011.

Sellers, P., Randall, D., Collatz, G., Berry, J., Field, C., Dazlich, D., Zhang, C., Collelo, G., and Bounoua, L.: A revised land surface parameterization (SiB2) for atmospheric GCMs. Part I: Model formulation, Journal of climate, 9, 676-705, 1996a.

Sellers, P. J., Tucker, C. J., Collatz, G. J., Los, S. O., Justice, C. O., Dazlich, D. A., and Randall, D. A.: A revised land surface parameterization (SiB2) for atmospheric GCMs. Part II: The generation of global fields of terrestrial biophysical parameters from satellite data, Journal of climate, 9, 706-737, 1996b.

Shen, M., Tang, Y., Chen, J., Zhu, X., and Zheng, Y.: Influences of temperature and precipitation before the growing season on spring phenology in grasslands of the central and eastern Qinghai-Tibetan Plateau, Agricultural and Forest Meteorology, 151, 1711-1722, 2011.

Thornton, P., Thornton, M., Mayer, B., Wilhelmi, N., Wei, Y., and Cook, R.: Daymet: Daily surface weather on a 1 km grid for North America, 1980-2008, Oak Ridge National Laboratory Distributed Active Archive Center, Oak Ridge, Tennessee, USA., 2012. 2012.

Turner, D. P., Ritts, W. D., Cohen, W. B., Gower, S. T., Running, S. W., Zhao, M., Costa, M. H., Kirschbaum, A. A., Ham, J. M., and Saleska, S. R.: Evaluation of MODIS NPP and GPP products across multiple biomes, Remote Sensing of Environment, 102, 282-292, 2006.

Urbanski, S., Barford, C., Wofsy, S., Kucharik, C., Pyle, E., Budney, J., McKain, K., Fitzjarrald, D., Czikowsky, M., and Munger, J.: Factors controlling CO2 exchange on timescales from hourly to decadal at Harvard Forest, Journal of Geophysical Research: Biogeosciences, 112, 2007.

White, M. A., Thornton, P. E., Running, S. W., and Nemani, R. R.: Parameterization and sensitivity analysis of the BIOME–BGC terrestrial ecosystem model: net primary production controls, Earth interactions, 4, 1-85, 2000.

Xiao, X., Zhang, Q., Braswell, B., Urbanski, S., Boles, S., Wofsy, S., Moore, B., and Ojima, D.: Modeling gross primary production of temperate deciduous broadleaf forest using satellite images and climate data, Remote Sensing of Environment, 91, 256-270, 2004.

Xiao, Z., Liang, S., Wang, J., Chen, P., Yin, X., Zhang, L., and Song, J.: Use of General Regression Neural Networks for Generating the GLASS Leaf Area Index Product From Time-Series MODIS Surface Reflectance, IEEE Transactions on Geoscience and Remote Sensing, 2014. 209-223, 2014.

Xie, J., Chen, J., Sun, G., Chu, H., Noormets, A., Ouyang, Z., John, R., Wan, S., and Guan, W.: Long-term variability and environmental control of the carbon cycle in an oak-dominated temperate forest, Forest Ecology and Management, 313, 319-328, 2014.

Xin, Q.: A risk-benefit model to simulate vegetation spring onset in response to multi-decadal climate variability: Theoretical basis and applications from the field to the Northern Hemisphere, Agricultural and Forest Meteorology, 228–229, 139-163, 2016.

Xin, Q., Dai, Y., Li, X., Liu, X., Gong, P., and Richardson, A. D.: A steady-state approximation approach to simulate seasonal leaf dynamics of deciduous broadleaf forests via climate variables, Agricultural and Forest Meteorology, 249, 44-56, 2018.

Yang, X., Mustard, J. F., Tang, J., and Xu, H.: Regional-scale phenology modeling based on meteorological records and remote sensing observations, Journal of Geophysical Research: Biogeosciences, 117, 2012.

Yu, C., Li, C., Xin, Q., Chen, H., Zhang, J., Zhang, F., Li, X., Clinton, N., Huang, X., Yue, Y., and Gong, P.: Dynamic assessment of the impact of drought on agricultural yield and scale-dependent return periods over large geographic regions, Environmental Modelling & Software, 62, 454-464, 2014.

Yuan, H., Dickinson, R. E., Dai, Y., Shaikh, M. J., Zhou, L., Shangguan, W., and Ji, D.: A 3D Canopy Radiative Transfer Model for Global Climate Modeling: Description, Validation, and Application, Journal of Climate, 27, 1168-1192, 2013.

Yuan, W., Liu, S., Yu, G., Bonnefond, J.-M., Chen, J., Davis, K., Desai, A. R., Goldstein, A. H., Gianelle, D., and Rossi, F.: Global estimates of evapotranspiration and gross primary production based on MODIS and global meteorology data, Remote Sensing of Environment, 114, 1416-1431, 2010.

Zeng, F., Collatz, G. J., Pinzon, J. E., and Ivanoff, A.: Evaluating and quantifying the climate-driven interannual variability in Global Inventory Modeling and Mapping Studies (GIMMS) Normalized Difference Vegetation Index (NDVI3g) at global scales, Remote Sensing, 5, 3918-3950, 2013.

Zhu, P., Zhuang, Q., Ciais, P., Welp, L., Li, W., and Xin, Q.: Elevated atmospheric CO2 negatively impacts photosynthesis through radiative forcing and physiology-mediated climate feedback, Geophysical Research Letters, 44, 1956-1963, 2017.